

AD-A035 851

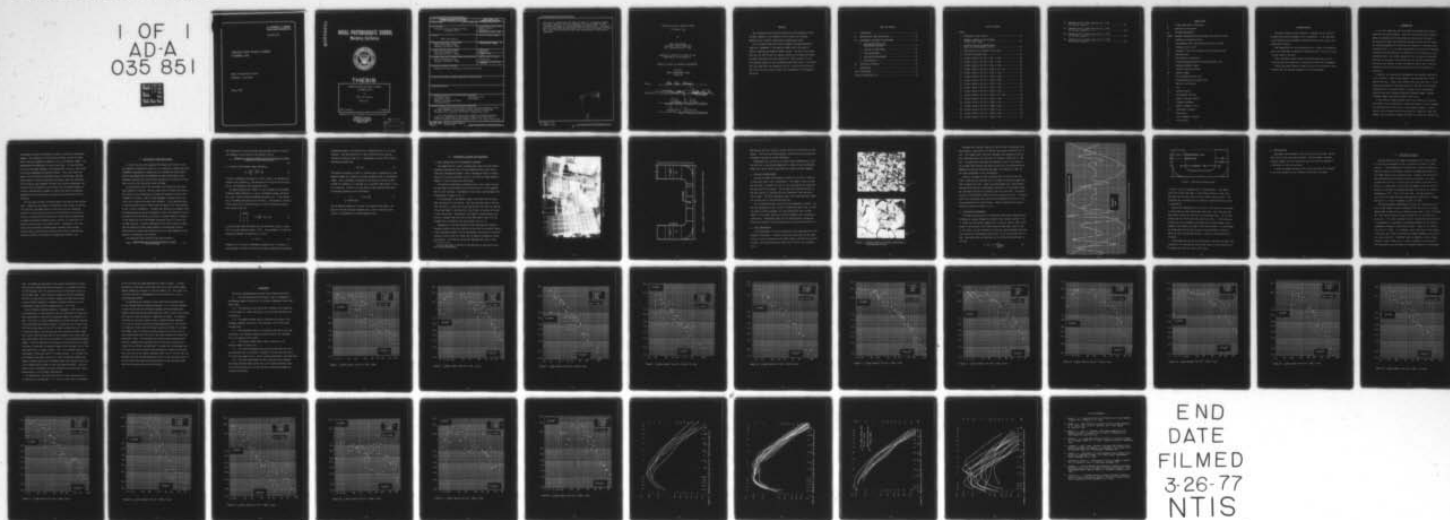
NAVAL POSTGRADUATE SCHOOL MONTEREY CALIF
TRANSVERSE FORCES ON ROUGH CYLINDERS IN HARMONIC FLOW.(U)
MAR 77 P J HENNING

F/G 20/4

UNCLASSIFIED

NL

1 OF 1
AD-A
035 851



U.S. DEPARTMENT OF COMMERCE
National Technical Information Service

AD-A035 851

TRANSVERSE FORCES ON ROUGH CYLINDERS
IN HARMONIC FLOW

NAVAL POSTGRADUATE SCHOOL
MONTEREY, CALIFORNIA

MARCH 1977

ADA035851

NAVAL POSTGRADUATE SCHOOL

Monterey, California



THESIS

TRANSVERSE FORCES ON ROUGH CYLINDERS
IN HARMONIC FLOW

by

Peter John Henning

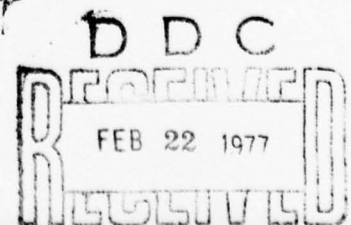
March 1977

Thesis Advisor:

T. Sarpkaya

Approved for public release; distribution unlimited.

REPRODUCED BY
NATIONAL TECHNICAL
INFORMATION SERVICE
U. S. DEPARTMENT OF COMMERCE
SPRINGFIELD, VA. 22161



| REPORT DOCUMENTATION PAGE | | READ INSTRUCTIONS BEFORE COMPLETING FORM |
|--|-----------------------|--|
| 1. REPORT NUMBER | 2. GOVT ACCESSION NO. | 3. RECIPIENT'S CATALOG NUMBER |
| 4. TITLE (and Subtitle) Transverse Forces on Rough Cylinders in Harmonic Flow | | 5. TYPE OF REPORT & PERIOD COVERED Master's Thesis; March 1977 |
| | | 6. PERFORMING ORG. REPORT NUMBER |
| 7. AUTHOR(s) Peter John Henning | | 8. CONTRACT OR GRANT NUMBER(s) |
| 9. PERFORMING ORGANIZATION NAME AND ADDRESS Naval Postgraduate School Monterey, California 93940 | | 10. PROGRAM ELEMENT, PROJECT, TASK AREA & WORK UNIT NUMBERS |
| 11. CONTROLLING OFFICE NAME AND ADDRESS Naval Postgraduate School Monterey, California 93940 | | 12. REPORT DATE March 1977 |
| | | 13. NUMBER OF PAGES 50 |
| 14. MONITORING AGENCY NAME & ADDRESS (if different from Controlling Office) Naval Postgraduate School Monterey, California 93940 | | 15. SECURITY CLASS. (of this report) Unclassified |
| | | 15a. DECLASSIFICATION/DOWNGRADING SCHEDULE |
| 16. DISTRIBUTION STATEMENT (of this Report) Approved for public release; distribution unlimited. | | |
| 17. DISTRIBUTION STATEMENT (of the abstract entered in Block 20, if different from Report) | | |
| 18. SUPPLEMENTARY NOTES | | |
| 19. KEY WORDS (Continue on reverse side if necessary and identify by block number) Transverse Forces Alternating Force Oscillatory Flow Wave Forces Harmonic Flow about Cylinders Lift Coefficient | | |
| 20. ABSTRACT (Continue on reverse side if necessary and identify by block number) The transverse forces acting on smooth and sand-roughened circular cylinders immersed in an harmonically oscillating flow have been measured using a recently constructed U-shaped water tunnel. The lift coefficients were found to depend on Keulegan-Carpenter number but independent of the Reynolds number within the range of relative roughness and Reynolds numbers tested. The results have shown | | |

that the lift coefficients for smooth cylinders at low Reynolds numbers are nearly identical with those obtained for rough cylinders at very high Reynolds numbers at the corresponding amplitude ratios. The results have also shown that the transverse force is a very significant fraction of the in-line force and must be taken into consideration in the design of structures.

| | |
|---------------|---|
| ACCESSION for | |
| NTIS | White Section <input checked="" type="checkbox"/> |
| DDI | Blue Section <input type="checkbox"/> |
| UNCLASSIFIED | |
| JUSTIFICATION | |
| BY | |
| DATE | |
| A | |

Transverse Forces on Rough Cylinders
in Harmonic Flow

by

Peter John Henning
Lieutenant, United States Navy
B.S., Lehigh University, 1969

Submitted in partial fulfillment of the
requirements for the degree of

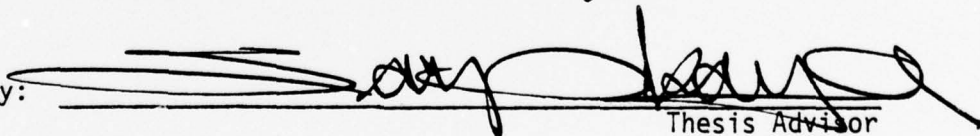
MASTER OF SCIENCE IN MECHANICAL ENGINEERING

from the
NAVAL POSTGRADUATE SCHOOL
March 1977

Author

Peter John Henning

Approved by:


Thesis Advisor

Allen E. Fuchs
Chairman, Department of Mechanical Engineering

Robert R. Fossum
Dean of Science and Engineering

ABSTRACT

The transverse forces acting on smooth and sand-roughened circular cylinders immersed in an harmonically oscillating flow have been measured using a recently constructed U-shaped water tunnel.

The lift coefficients were found to depend on Keulegan-Carpenter number but independent of the Reynolds number within the range of relative roughness and Reynolds numbers tested. The results have shown that the lift coefficients for smooth cylinders at low Reynolds numbers are nearly identical with those obtained for rough cylinders at very high Reynolds numbers at the corresponding amplitude ratios. The results have also shown that the transverse force is a significant fraction of the in-line force and must be taken into consideration in the design of structures.

TABLE OF CONTENTS

| | | |
|------|---|----|
| I. | INTRODUCTION - - - - - | 10 |
| II. | DEFINITION OF FORCE COEFFICIENTS - - - - - | 12 |
| III. | EXPERIMENTAL EQUIPMENT AND PROCEDURES - - - - - | 15 |
| | A. BRIEF DESCRIPTION OF THE EXPERIMENTAL EQUIPMENT - - - - - | 15 |
| | B. CIRCULAR CYLINDER MODELS - - - - - | 18 |
| | C. FORCE MEASUREMENTS - - - - - | 18 |
| | D. ACCELERATION MEASUREMENTS - - - - - | 20 |
| | E. DATA REDUCTION - - - - - | 23 |
| IV. | DISCUSSION OF RESULTS - - - - - | 24 |
| V. | CONCLUSIONS - - - - - | 27 |
| | LIST OF REFERENCES - - - - - | 49 |
| | INITIAL DISTRIBUTION LIST - - - - - | 50 |

LIST OF FIGURES

Figure

| | |
|--|----|
| 1. Photograph of the U-tunnel - - - - - | 16 |
| 2. Schematic drawing of the U-shaped vertical water tunnel - - - - - | 17 |
| 3. Scanning electron microscope photo- graphs of sand-roughened surface - - - - - | 19 |
| 4. Acceleration and transverse force traces - - - - - | 21 |
| 5. Position of pressure taps - - - - - | 22 |
| 6. $C_L(\max)$ versus K for $k/D = 1/50$, 3 inch - - - - - | 28 |
| 7. $C_L(\max)$ versus K for $k/D = 1/50$, 6 inch - - - - - | 29 |
| 8. $C_L(\max)$ versus K for $k/D = 1/100$, 2 inch - - - - - | 30 |
| 9. $C_L(\max)$ versus K for $k/D = 1/100$, 2 1/2 inch - - - - - | 31 |
| 10. $C_L(\max)$ versus K for $k/D = 1/100$, 3 inch - - - - - | 32 |
| 11. $C_L(\max)$ versus K for $k/D = 1/100$, 4 inch - - - - - | 33 |
| 12. $C_L(\max)$ versus K for $k/D = 1/100$, 5 inch - - - - - | 34 |
| 13. $C_L(\max)$ versus K for $k/D = 1/100$, 6 inch - - - - - | 35 |
| 14. $C_L(\max)$ versus K for $k/D = 1/100$, 7 inch - - - - - | 36 |
| 15. $C_L(\max)$ versus K for $k/D = 1/200$, 2 inch - - - - - | 37 |
| 16. $C_L(\max)$ versus K for $k/D = 1/200$, 2 1/2 inch - - - - - | 38 |
| 17. $C_L(\max)$ versus K for $k/D = 1/200$, 3 inch - - - - - | 39 |
| 18. $C_L(\max)$ versus K for $k/D = 1/800$, 3 inch - - - - - | 40 |
| 19. $C_L(\max)$ versus K for $k/D = 1/800$, 4 inch - - - - - | 41 |
| 20. $C_L(\max)$ versus K for $k/D = 1/800$, 5 inch - - - - - | 42 |
| 21. $C_L(\max)$ versus K for $k/D = 1/800$, 6 inch - - - - - | 43 |
| 22. $C_L(\max)$ versus K for $k/D = 1/800$, 7 inch - - - - - | 44 |

23. Combined plot of $C_L(\max)$ data for $k/D = 1/50$
for various values of β - - - - - - - - - - -45
24. Combined plot of $C_L(\max)$ data for $k/D = 1/100$
for various values of β - - - - - - - - - - -46
25. Combined plot of $C_L(\max)$ data for $k/D = 1/200$
for various values of β - - - - - - - - - - -47
26. Combined plot of $C_L(\max)$ data for $k/D = 1/800$
for various values of β - - - - - - - - - - -48

NOMENCLATURE

| | |
|------------|--|
| A | Virtual amplitude of the motion |
| A_1 | Amplitude of the motion |
| a_m | Maximum acceleration |
| CLMAX | Maximum transverse force coefficient, also used as $C_L(\max)$ |
| D | Diameter of the test cylinder |
| F | Instantaneous total force acting on the test cylinder |
| f_r | Frequency ratio, $f_v/1/T$ |
| f_v | Frequency of the first harmonic of the transverse force |
| F_m | Measured force |
| g | Gravitational acceleration |
| H | Distance between pressure taps and mean water level |
| K | Keulegan-Carpenter number |
| L | Length of the test cylinder |
| Re | Reynolds number |
| k | Sand roughness particle size |
| s | Distance between the pressure taps |
| T | Period of oscillations |
| t | Time |
| U_m | Maximum velocity |
| u | Instantaneous velocity |
| w | Width of the test section |
| β | Frequency parameter |
| γ | Specific weight of fluid |
| ΔP | Differential pressure |
| θ | Phase angle |
| ν | Fluid kinematic viscosity |
| ρ | Fluid density |

ACKNOWLEDGEMENTS

The author wishes to thank Professor T. Sarpkaya for his continual guidance and patience throughout this investigation. It has been both a privilege and a most worthwhile experience to work with a man of such professional stature.

Great appreciation is also expressed to Mr. J. McKay of the Machine Shop in the Department of Mechanical Engineering who is truly an artisan in every sense of the word.

Also, the author wishes to thank the United States Navy for providing me with this opportunity to further my professional development.

Finally the author wishes to thank his wife for the continual understanding that she provides regardless of the circumstances.

I. INTRODUCTION

It is a well known fact that flow about bluff bodies gives rise to separation and vortex shedding. Aside from the fact that the formation, growth, and shedding of vortices produce a drag force on the body in the direction of mean flow (hereafter referred to as the in-line force), the alternate shedding of the vortices also results in a time-dependent transverse force. It is of both fluid-dynamical and practical importance to evaluate the amplitude and the frequency of all the harmonics of the transverse force. The primary reasons for this are that the transverse force may set the body in motion resulting in a so-called hydroelastic oscillation and fatigue, and that the vectorial sum of the in-line and transverse force may be the most important force for the design of a structure.

Evidently, the transverse force depends on the shedding characteristics of vortices. These in turn depend on the characteristics of the ambient flow (e.g. steady flow, harmonic flow, wavy flow, etc.), on the shape and orientation of the body relative to the flow, on the surface characteristics of the body (smooth or rough), and on the parameters characterizing the fluid-body interaction (Reynolds number, Keulegan-Carpenter number, wave height to depth ratio, etc.).

Of the scores of papers written on the fluid loading on structures, none seems to have systematically treated the effect of surface roughness on transverse force, particularly at high Reynolds numbers. Previous studies, such as those carried out by Chang [1], Bidde [2], Wiegel and Delmonte [3], Mercier [4], Sarpkaya and Tuter [5], Jones [6], Isaacson [7],

and Sarpkaya [8] dealt with smooth cylinders at relatively low Reynolds numbers. Only recently, Collins [9] has conducted a series of experiments with sand-roughened cylinders at fairly high Reynolds numbers and demonstrated the importance of surface conditions. The data obtained by Collins have been extended in the present work to cover a wider range of relative roughnesses and Reynolds numbers. Thus, the primary purposes of this continuing investigation were to furnish data, obtained under carefully controlled laboratory conditions, about the transverse force acting on sand-roughened cylinders with relative roughnesses from $1/800$ to $1/50$ in harmonically oscillating fluid at Reynolds numbers up to about 1,000,000 and to attempt to identify the physical mechanisms responsible for the correlation or scatter of the transverse force coefficient.

This work does not deal with ocean waves or wave and current combinations. Therefore, the effects of diffraction, free surface, or varying fluid velocity with depth along a vertical pile are not considered. Suffice it to note that the variation of the direction of the velocity vector at a given point with time and at a given time with depth tends to reduce the spanwise coherence along a vertical pile resulting in a reduced in-line as well as transverse force. Consequently, the transverse force coefficients presented herein represent their maximum possible value since they have resulted from a highly correlated wake along the cylinder in a perfectly two-dimensional harmonic flow.

II. DEFINITION OF FORCE COEFFICIENTS

In view of the fact that separated flow about bluff bodies is not yet amenable to theoretical analysis, it is necessary to obtain the force components experimentally through the use of appropriate coefficients. One can then demonstrate the dependence of these coefficients on the parameters governing the flow and give some sense of universality to the data as well as the conclusions drawn from them.

As pointed out earlier, the transverse force stems from the alternate shedding of vortices. During a given cycle of harmonic oscillation the velocity varies sinusoidally and hence the strength as well as the frequency of vortices. Thus, the time dependent transverse force contains first, second, and higher order harmonics. A very detailed study of the transverse force will require the evaluation of all the harmonics as well as their frequencies. Evidently this would be an extremely time-consuming process and would not necessarily add to the designer's ability to predict the forces acting on pilings to a greater degree of accuracy. In the present work only the maximum transverse force in a given cycle has been analyzed. A cursory examination of the force traces has shown that the second and higher order harmonics are considerably smaller. These second and higher order harmonics may be of some importance in the analysis of hydroelastic oscillations.

The transverse force coefficient has been defined by:

$$CL_{MAX} = \frac{\text{maximum peak of the transverse force in a cycle}}{(.5)(\rho)(D)(L)(U_m^2)} \quad (1)$$

The frequencies of oscillation have been expressed either in terms of the frequency of oscillation of the harmonic flow as

$$f_r = \frac{\text{frequency of the first harmonic of the lift force in a cycle}}{\text{frequency of the harmonic motion}} \quad (2)$$

or in terms of the Strouhal number defined by

$$St = \frac{f_v D}{U_m} = \frac{f_v / f}{k} = \frac{f_r}{k} \quad (3)$$

in which ρ represents the density of fluid; D and L , the diameter and length of the cylinder; U_m , the amplitude of the oscillating velocity; and f_v , the frequency of the transverse force.

As shown previously [9], CLMAX, St , and f_r depend on the Keulegan-Carpenter number defined by $K = U_m T / D$, the Reynolds number defined by $Re = U_m D / \nu$, and the relative roughness defined by k/D . In the foregoing, T represents the period of oscillation; ν , the kinematic viscosity of the fluid; and k , the mean height of carefully-sieved sand grains. Thus one may write [9]:

$$\begin{Bmatrix} CLMAX \\ f_r \\ St \end{Bmatrix} = f_i \left(\frac{U_m T}{D}, Re, k/D \right) \quad (4)$$

It has also been shown previously [9] that either Re or $U_m T / D$ in equation (4) may be replaced by $Re/K = D^2 / \nu T$. This parameter is called the frequency parameter and denoted by β , so that

$$\beta = D^2 / \nu T \quad (5)$$

Evidently, for a series of experiments conducted with a cylinder of a given diameter in water (of uniform and constant temperature and density)

undergoing harmonic oscillations with a constant period (T), β is held constant. Then the variation of a force coefficient with K may be plotted for constant values of β . Subsequently, one can easily recover the Reynolds number from

$$Re = \beta K \quad (6)$$

and connect the points, on each $\beta = \text{constant}$ curve, representing a given Reynolds number for a family of suitably selected values of the Reynolds number. Such a procedure eliminates the difficulty of trying to draw contours of constant K , or constant Re , or constant CL_{MAX} versus K or Re or K versus Re . Suffice it to note that the data reported herein shall be analyzed according to the relationship

$$C_i = f_i(K, \beta, \frac{k}{D}) \quad (7)$$

[a coefficient]

and the Reynolds number will be used in the manner cited above. The power of this new plotting procedure (new, as far as the wave force analysis is concerned) will become apparent later.

III. EXPERIMENTAL EQUIPMENT AND PROCEDURES

A. BRIEF DESCRIPTION OF THE EXPERIMENTAL EQUIPMENT

The capabilities of a small U-shaped water tunnel have been demonstrated by Sarpkaya and Tuter [5] for generating oscillatory flow at relatively low Reynolds numbers. When it became desirable to investigate the in-line and transverse forces on cylinders at higher Reynolds numbers, a larger U-tunnel was constructed.

The design and operational characteristics of this larger U-tunnel are described in great detail by Collins [9] and will not be repeated here in their entirety. A photograph of the tunnel used throughout this investigation is shown in Fig. 1.

Of significance is the general shape of the tunnel and its effect upon the velocity of oscillation. The cross sectional area of the two legs (6x3 feet) is twice that of the test section (3x3 feet) so that the virtual amplitude* or the velocity of oscillation is exactly twice that of the free surface. Additionally, the length of the horizontal test section is greater than twice the virtual amplitude so that fully developed flow is achieved in the test section (see Fig. 2).

Compressed air and four butterfly valves (operated by a pneumatic three-way control valve) were used to set the fluid into harmonic motion. It was considered prudent to allow the harmonic oscillations to damp out naturally during a test run rather than to employ the method of forced oscillations. The butterfly valves were operated only once, at the

*Virtual amplitude is defined as the amplitude of oscillation which the cylinder experiences.

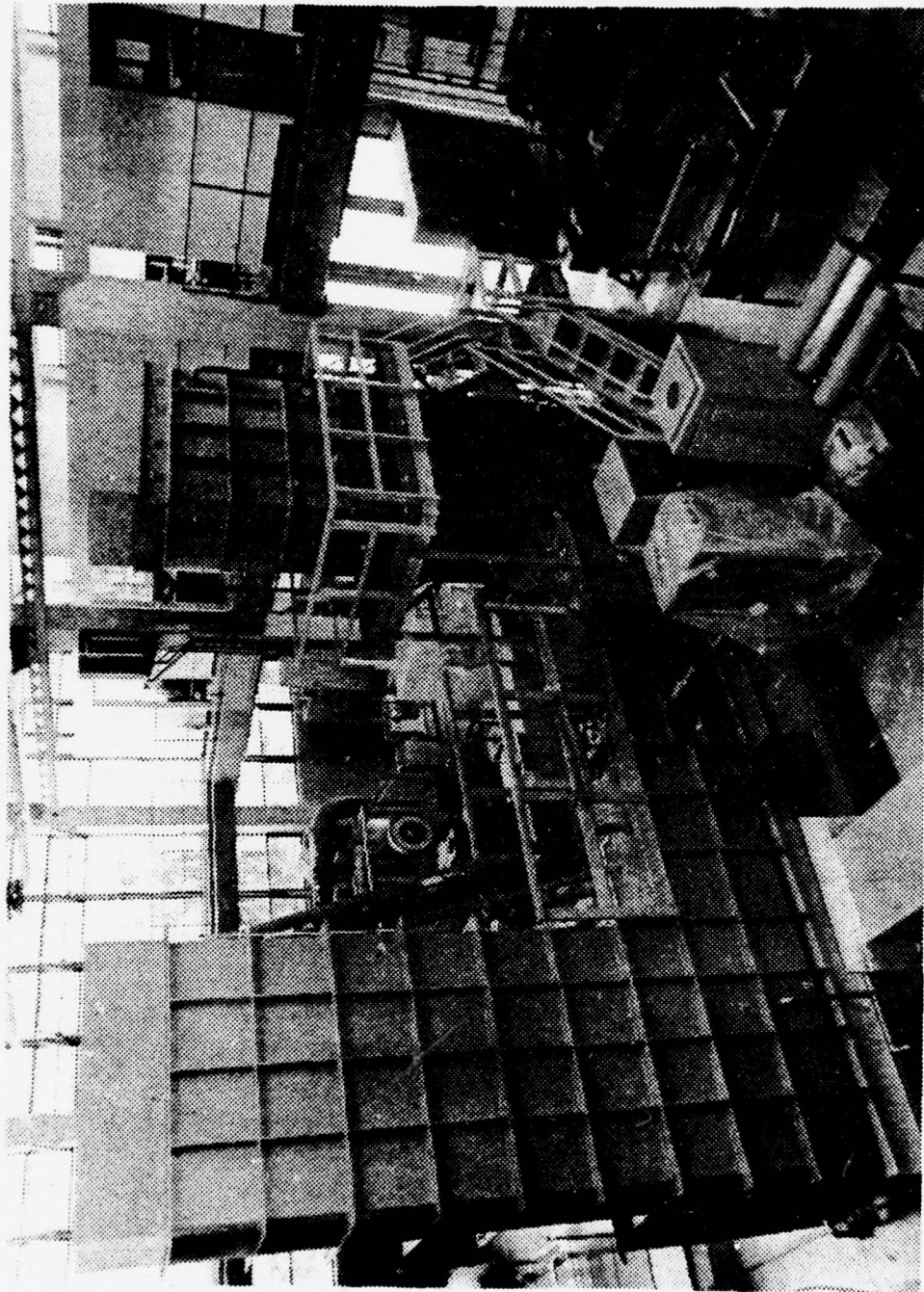


Figure 1. Photograph of the U-tunnel.

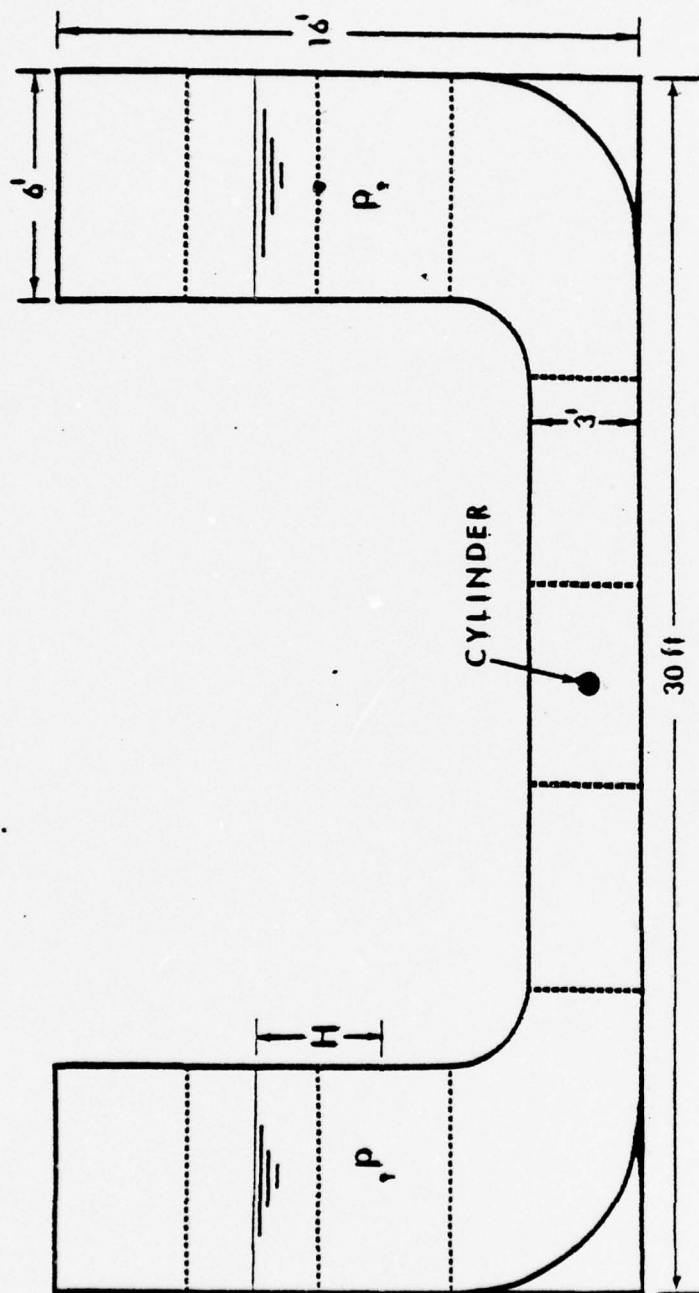


Figure 2. Schematic drawing of the U-shaped vertical water tunnel.

beginning of each run, causing a natural period of oscillation of 5.507 seconds. The fluid oscillated smoothly, and the force and acceleration transducers required no filters whatsoever.

Experiments were carried out at various water temperatures by heating the fluid to the desired temperature in order to vary the Reynolds number for a given relative amplitude and relative surface roughness.

B. CIRCULAR CYLINDER MODELS

Circular cylinders with diameters ranging in size from 7 inches to 2 inches were used in this investigation. The length of each cylinder was such that it allowed for a gap of 1/32 inch between the tunnel wall and each end of the cylinder. The cylinders were mounted and held in the test section by inserting the force transducers into each end of the cylinder. The force transducers used in this operation were identical to those used in the previous study [9].

This investigation dealt solely with sand-roughened cylinders. The sand was segregated by use of sieves of appropriate mesh sizes, so that the proper relative roughness, k/D , was achieved for each cylinder tested. This process resulted in uniform roughness which surpassed all expectations. Photographs taken with a scanning electron microscope show the uniformity of size and packing of the sand grains (see Fig. 3).

C. FORCE MEASUREMENTS

The instantaneous in-line and transverse forces were measured by two identical transducers. A special housing was fabricated for each gage so that it could be mounted on the tunnel window, inserted into the test cylinder, and rotated to measure either the in-line or the transverse force.



$k = 0.018''$
20-X



$k = 0.018''$
50-X

Figure 3. Scanning electron microscope photographs of sand-roughened surface.

The gages had a nominal capacity of 500 lbf with a 200 percent overload capacity. Application of a 500 lbf load caused a deflection of .01 inch. The largest actual load that the gages were subjected to during this investigation was less than 200 lbf, causing a deflection of .008 inch. The gages were calibrated by suspending a load in the middle of the cylinder after setting each gage to sense only the transverse force. Repeated calibrations have shown the gages to be perfectly linear for the loads encountered in the investigation.

Normally, one gage was used to measure the in-line force and the other to measure the transverse force, although at times both gages were used to measure only one. These force measurements were simultaneously recorded along with the instantaneous acceleration on two-channel Honeywell recorders operating at a speed of one inch per second. The natural period of 5.507 seconds allowed for 55.07 divisions per cycle. The amplitude of the transverse force and the flow characteristics such as K and Re were determined from these traces. Sample transverse force and acceleration traces are shown in Fig. 4.

D. ACCELERATION MEASUREMENTS

The method used during this investigation consisted of measuring the differential pressure between two pressure taps located as shown in Fig. 5. These taps were placed symmetrically on the two vertical legs of the tunnel at an elevation of 50 inches below the mean water level so that $H = 38$ inches. By use of Bernoulli's equation, applied between each pressure tap and the instantaneous water level, it can be shown that the virtual amplitude (twice the amplitude of the free surface amplitude) is given by:

$$A = 2A_1 = \frac{\Delta P / \gamma}{1 - \frac{1}{g} \left(\frac{2\pi}{T} \right)^2 H} \quad (8)$$

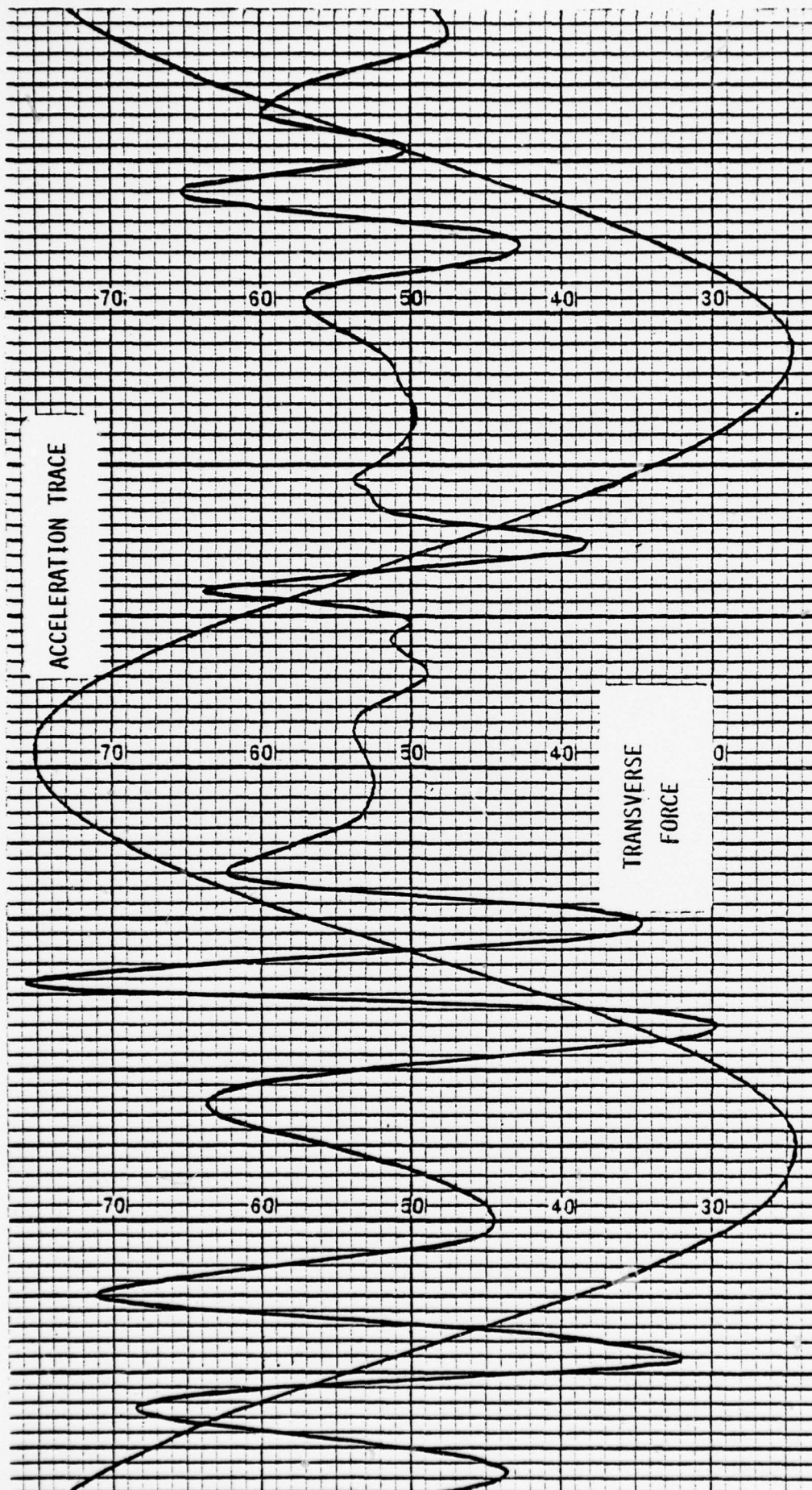


Figure 4. Acceleration and transverse force traces.

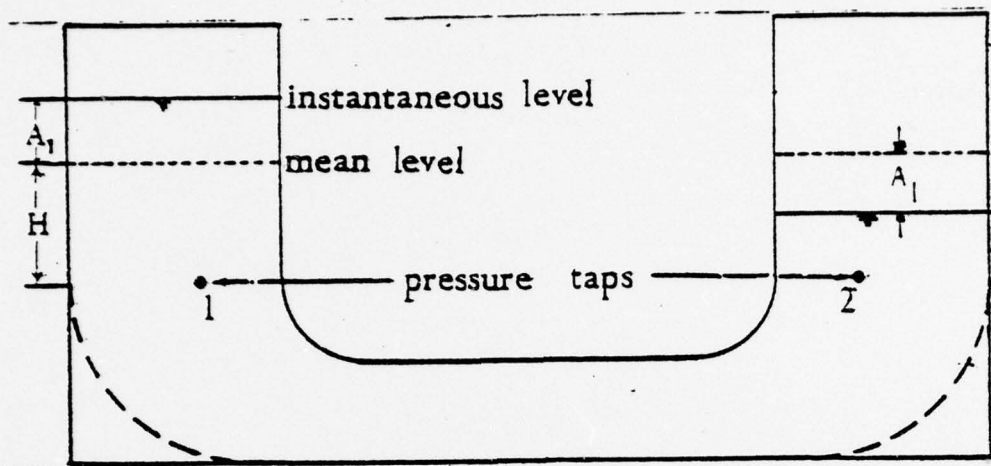


Figure 5. Position of pressure taps.

in which T and g are constant and H is kept constant. This method yields the virtual amplitude, or the maximum velocity in each cycle. The signal was entirely free of noise or small surface effects. The transducer was calibrated and its linearity checked before each series of experiments.

Because this measurement is so critical, the accuracy of the method just described has been checked many times over. Each time the alternate method verified the accuracy of the procedure used. Two of these methods used for verification are described in [9]. A third check was provided by using a magnetic velocimeter which sensed changes in the magnetic field caused by changes in the fluid velocity. As anticipated, the probe again verified the accuracy of the differential pressure method to within two percent accuracy, claimed by the manufacturer of the probe.

These comparisons as well as the perfectly sinusoidal and noise free character of all pressure and force traces speak for the suitability of the unique test facility used in this study.

E. DATA REDUCTION

Experiments were repeated at least twice for each cylinder, and normally both of these runs were evaluated. Reynolds number, Keulegan-Carpenter number, and lift coefficient were calculated for between 20 to 25 cycles for each run evaluated.

It should be emphasized again that only the amplitude and frequency of the first harmonic of the transverse forces were calculated.

IV. DISCUSSION OF RESULTS

The data obtained in the present investigation for various values of β and k/D are presented in Figs. 6 through 22 in terms of $C_L(\max)$ versus K . A close examination of the data for a given k/D ratio and β shows that there is considerable scatter in the data due primarily to the random nature of the transverse force. Secondly, the variation of the transverse-force coefficient from one β to another, for a given cylinder and k/D ratio, is no more than the scatter in the data for a given β . In other words, $C_L(\max)$ does not depend, within the limits of accuracy of the data, on the Reynolds number particularly for relative roughnesses of $k/D = 1/50$, $1/100$, and $1/200$. The data obtained by Collins [9] also show that the transverse-force coefficient is independent even for a relative roughness as small as $1/400$.

The Reynolds-number independence of $C_L(\max)$ for rough-walled cylinders, in the range of relative roughness from $1/400$ to $1/50$, is better demonstrated through the use of composite plots shown in Figs. 23 through 25. Each figure contains all data obtained with all cylinders for a given k/D . It is clearly apparent that the transverse-force coefficient is independent of β and hence of the Reynolds number for the relative roughnesses indicated in these three figures. Figure 26 is a similar plot for $k/D = 1/800$. It is apparent, within the limits of the scatter of the data, that there is some Reynolds number dependence, particularly for large values of β . Additional data are needed at relative roughnesses of $1/600$, $1/1000$, etc., in order to establish the variation of the transverse-force coefficient with Reynolds number as k/D approaches

zero. No attempt has been made in the present investigation to establish the said relationship primarily because it is extremely difficult to find and apply very fine sand particles with sufficient accuracy on the cylinders used. From a practical viewpoint, relative roughnesses as small as $1/800$ are not of special interest since the marine growth on the structural elements of offshore structures often give rise to considerably larger relative roughnesses (e.g. $k/D = 100$).

One of the most remarkable effects of roughness on the transverse force coefficient is the increase of the said coefficient to values commonly encountered at relatively low Reynolds numbers with smooth cylinders. This point is clearly demonstrated by plotting the mean transverse force coefficient for smooth cylinders at relatively low β values on the lift-force traces shown in Fig. 25 for rough cylinders with $k/D = 1/200$. It should be noted in passing that any one of the three figures, namely Figs. 23-25, could have been used for this purpose since $C_L(\max)$ does not vary significantly from one k/D to another for a given Keulegan-Carpenter number. Figure 25 shows that the transverse force coefficient for smooth cylinders at relatively low Reynolds numbers forms the upper limit of the same coefficient for rough cylinders. This is an extremely important experimental finding particularly for model testing. It is evident from the foregoing that tests carried out at very low Reynolds numbers with smooth cylinders should yield information about the transverse force acting on rough-walled cylinders at very high Reynolds numbers. The existence of such a relationship has been surmised but has never been clearly demonstrated as in the present investigation.

As noted earlier, the alternating nature of the transverse force is as important as its magnitude. It is for this reason that the frequency

of the lift force has been determined for rough cylinders. A careful examination of the results have shown that f_v/K or the Strouhal number remains essentially constant at a value of about 0.22. This result confirms that arrived at independently by Collins [9] and will not be elaborated upon further.

In considering the relevance of the coefficients presented herein to wave induced loads on offshore structures, it is of course important to take into account the differences between uniform two-dimensional harmonic motion and the wave motion where the velocity vector both rotates with time at a point and decays in magnitude with depth. The spanwise variations of the flow in general lead to reduced spanwise coherence. It is safe to assume that both the three-dimensionality of the flow and the reduction of the correlation length along the cylinder, in an ocean environment, tend to increase the base pressure and thus give rise to force coefficients which are smaller than those obtained with purely two-dimensional flows. The transverse force coefficients presented herein obviously represent their maximum possible values since they have resulted from a uniform, two-dimensional flow where the instantaneous wake of the cylinder has the highest possible degree of spanwise correlation. Thus, the value of the results presented herein lies in the fact that the designer now knows the maximum possible values of the transverse force if not the values which might be more appropriate to the conditions under which the structure must survive and function.

V. CONCLUSIONS

The results presented herein warrant the following conclusions:

(i) The transverse-force coefficient is nearly independent of the Reynolds number, particularly for relative roughnesses larger than about $1/800$;

(ii) The transverse force coefficient increases with increasing K in the range of K values from about 5 to 12 and then decreases with increasing K ;

(iii) The smooth cylinder data at relatively low values of the frequency parameter form more or less the upper limit of the rough cylinder data;

(iv) The transverse force is a significant fraction of the total resistance at all Reynolds numbers and must be taken into consideration in the design of structures;

(v) The Strouhal number remains nearly constant for all Reynolds numbers at about 0.22;

(vi) The results presented herein and the conclusions arrived at are applicable only to cylinders in harmonic flow with zero mean velocity within the range of Re , K , and k/D values encountered in the tests; and

(vii) The force coefficients for wavy flows may differ somewhat from those presented herein partly due to the reduced coherence along the cylinder and partly due to the nonlinear interaction between the current and the waves.

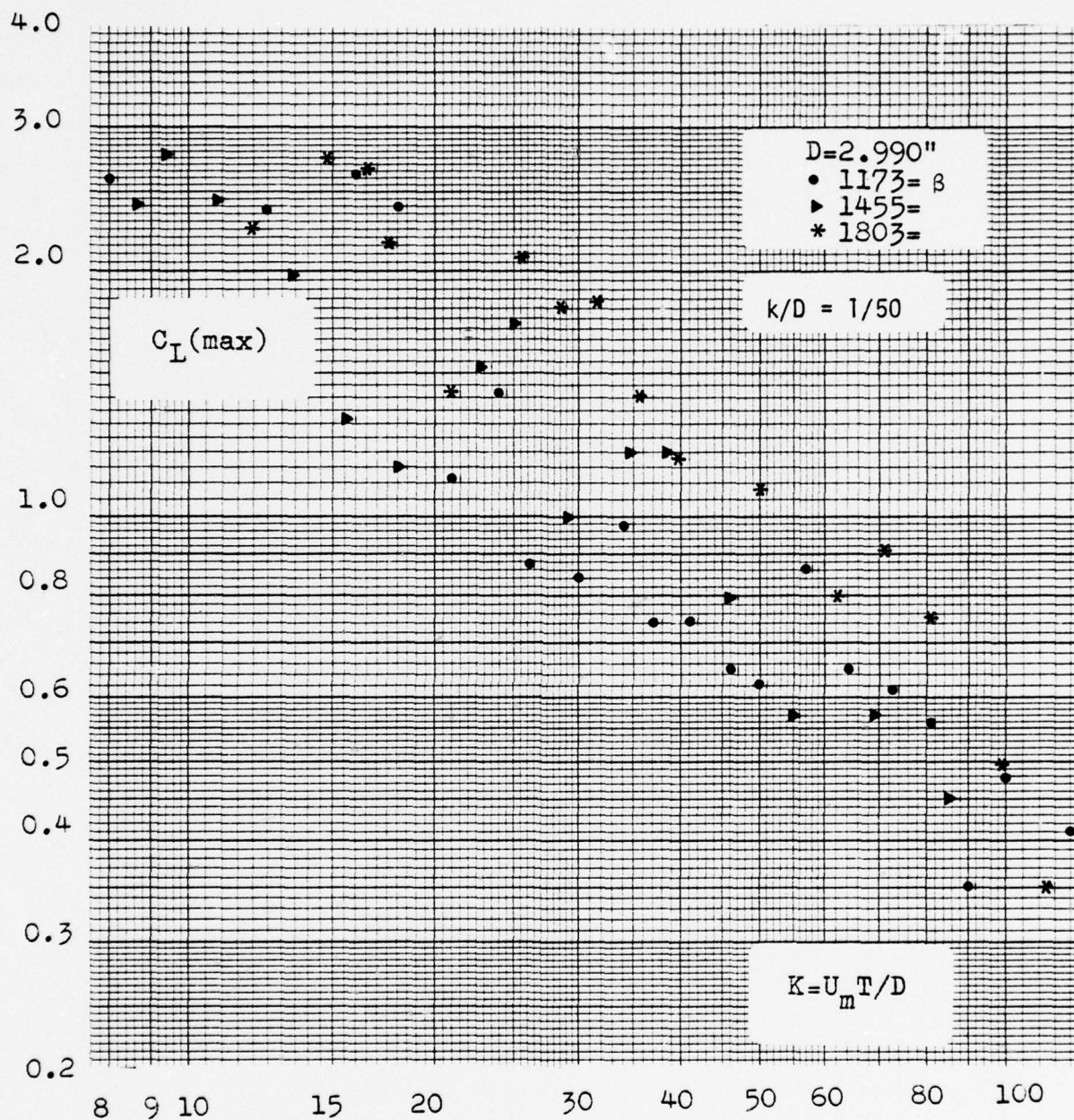


Figure 6. $C_L(\max)$ versus K for $k/D = 1/50$, 3 inch.

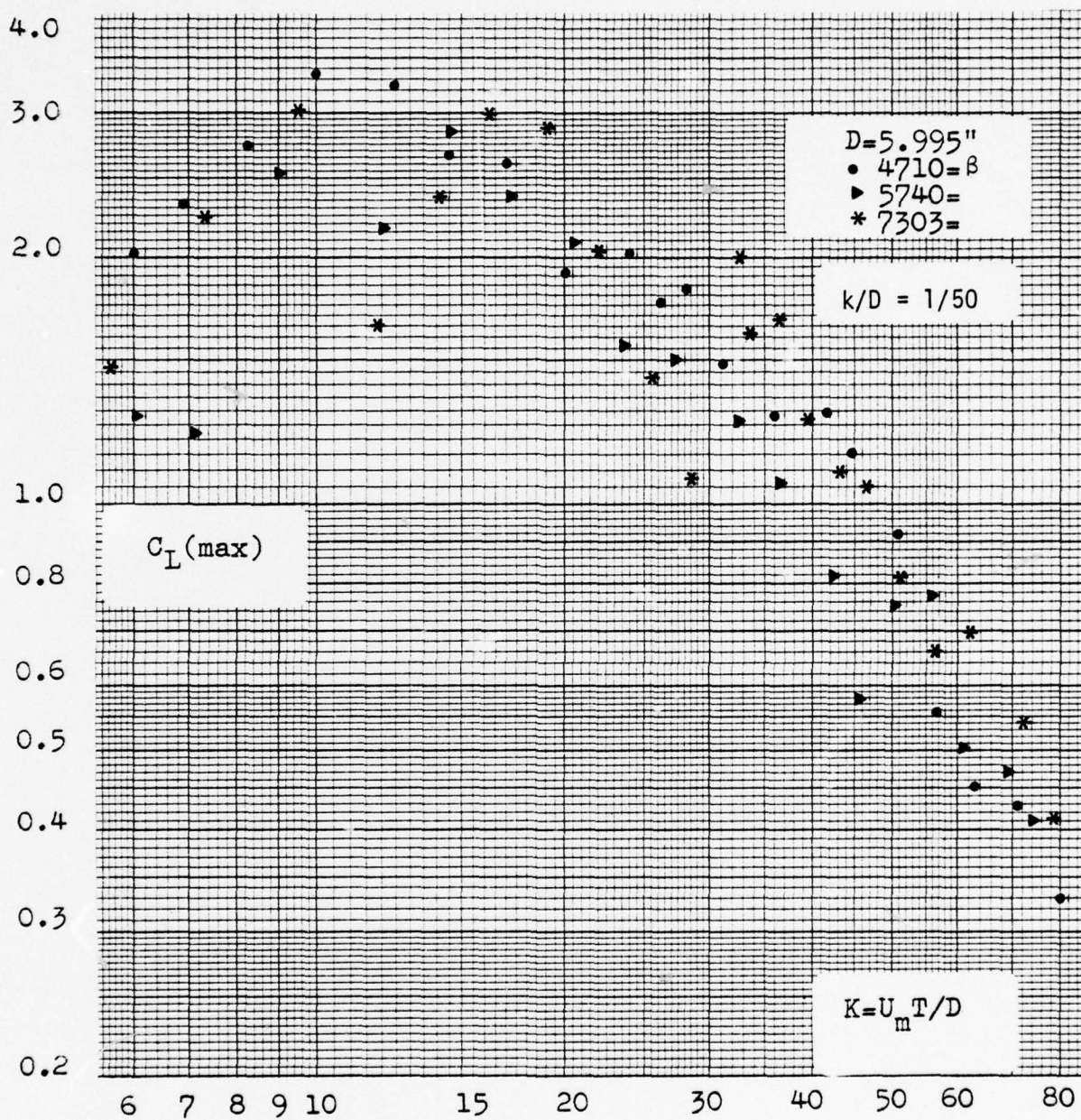


Figure 7. $C_L(\max)$ versus K for $k/D = 1/50$, 6 inch.

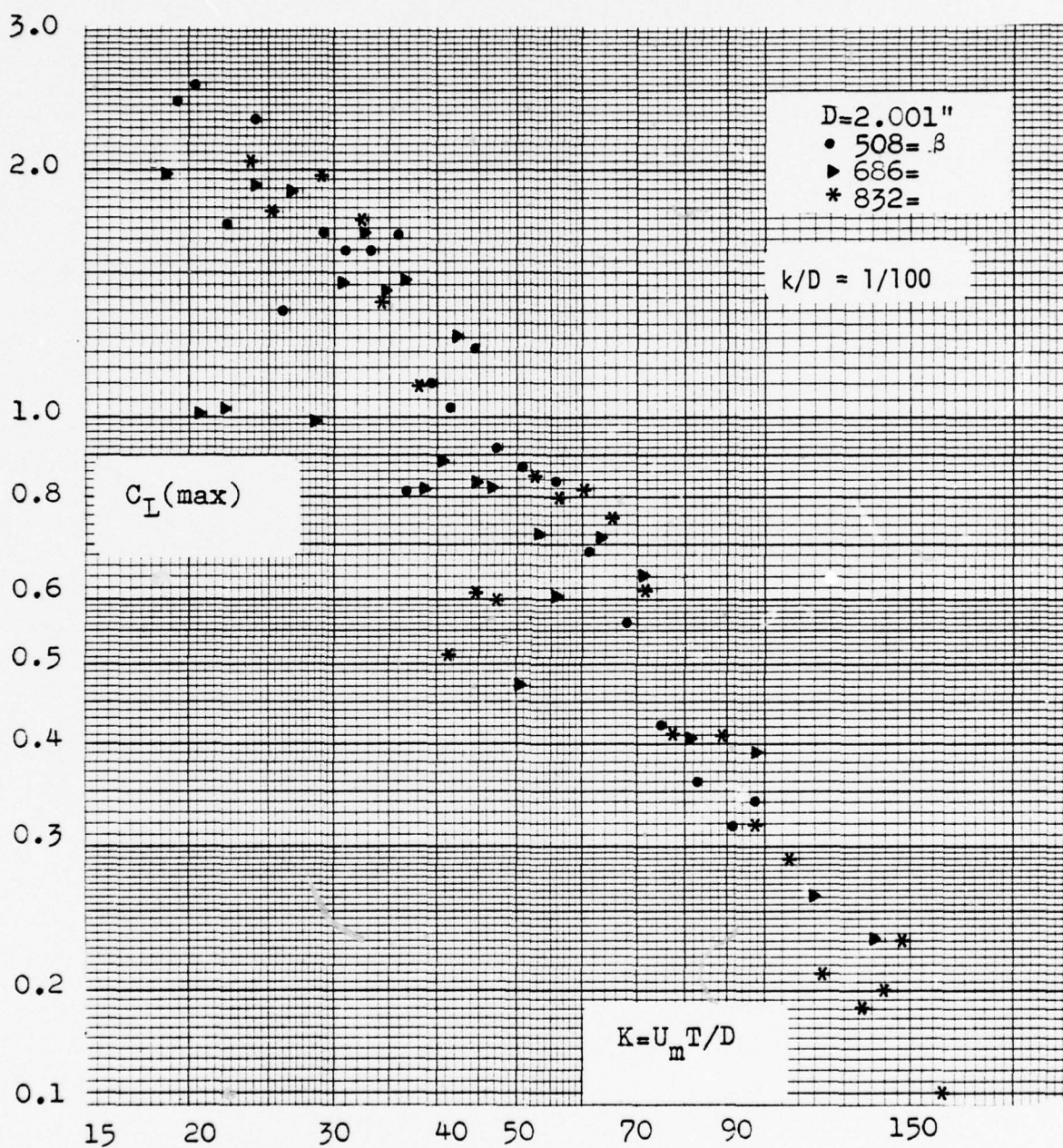


Figure 8. $C_L(\max)$ versus K for $k/D = 1/100$, 2 inch.

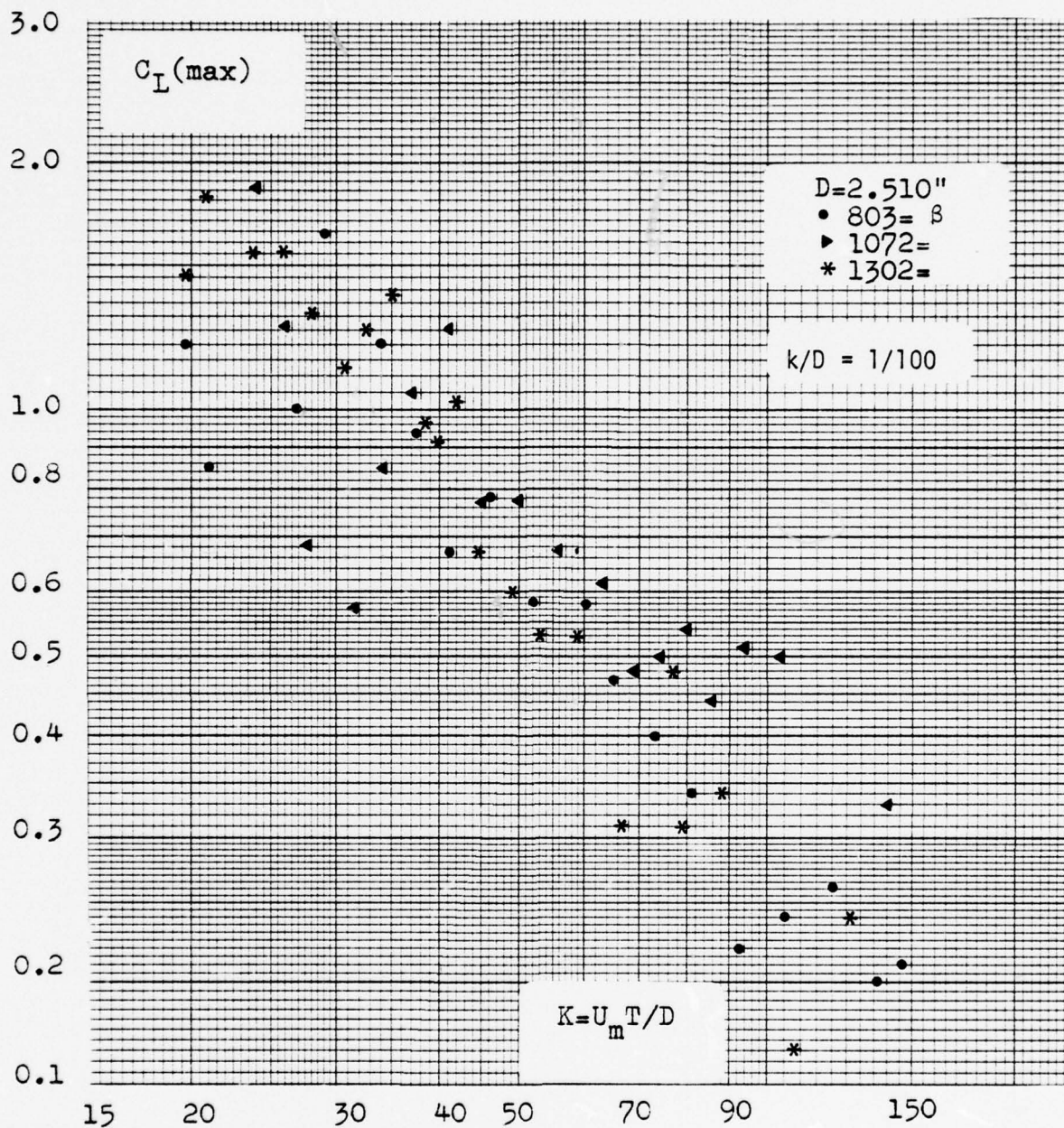


Figure 9. $C_L(\max)$ versus K for $k/D = 1/100$, 2 1/2 inch.

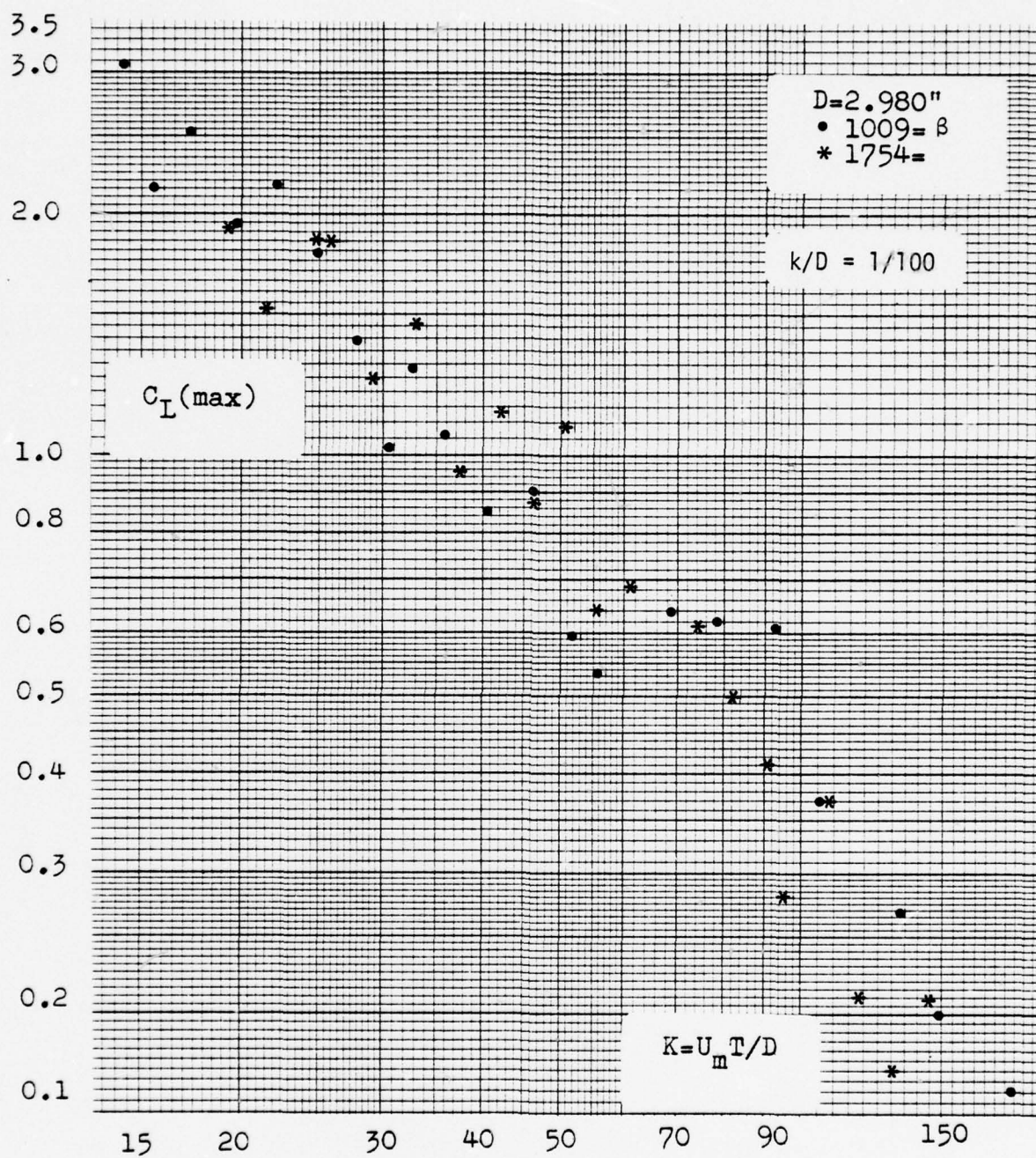


Figure 10. $C_L(\max)$ versus K for $k/D = 1/100$, 3 inch.

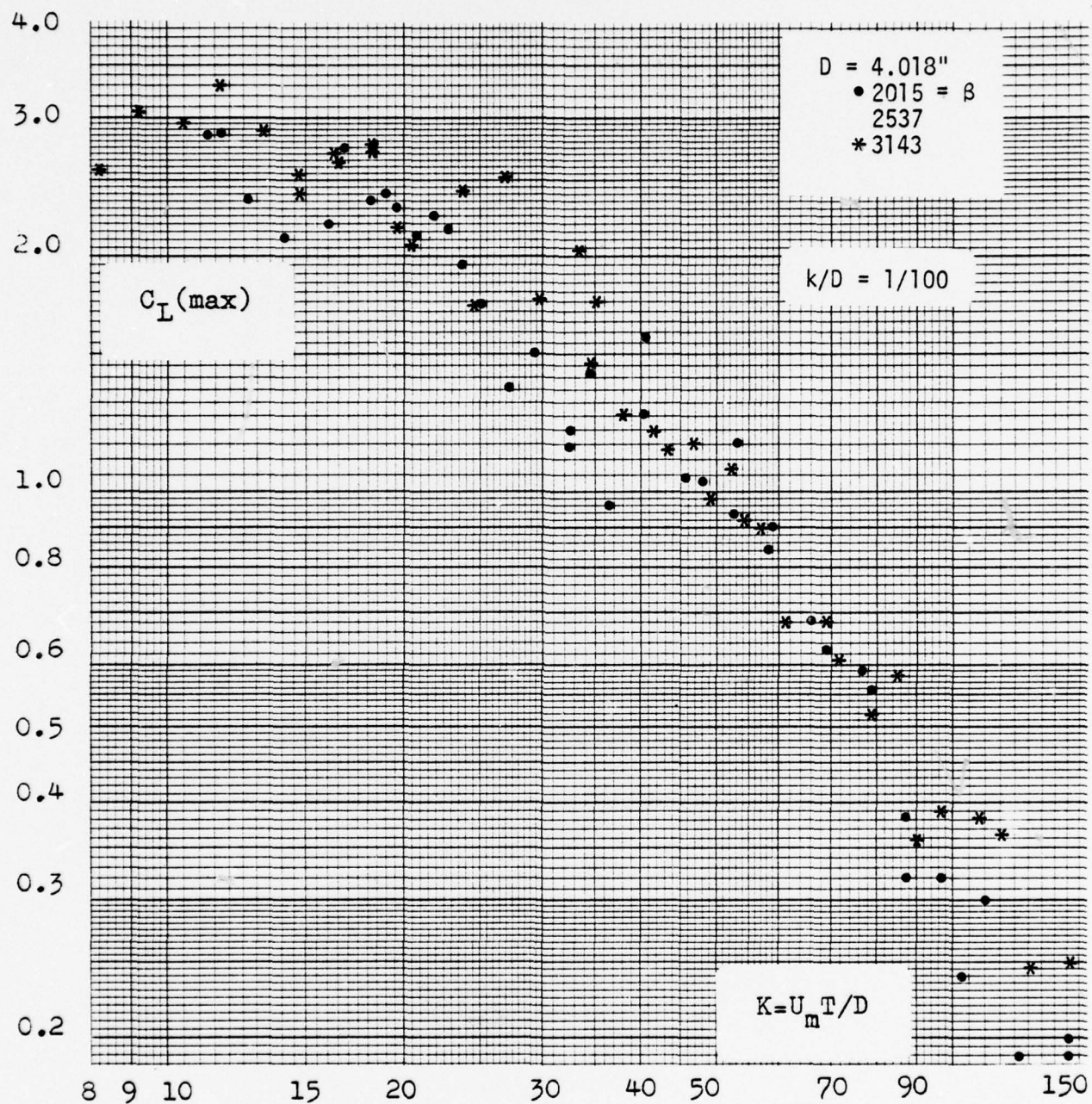


Figure 11. $C_L(\max)$ versus K for $k/D = 1/100$, 4 inch.

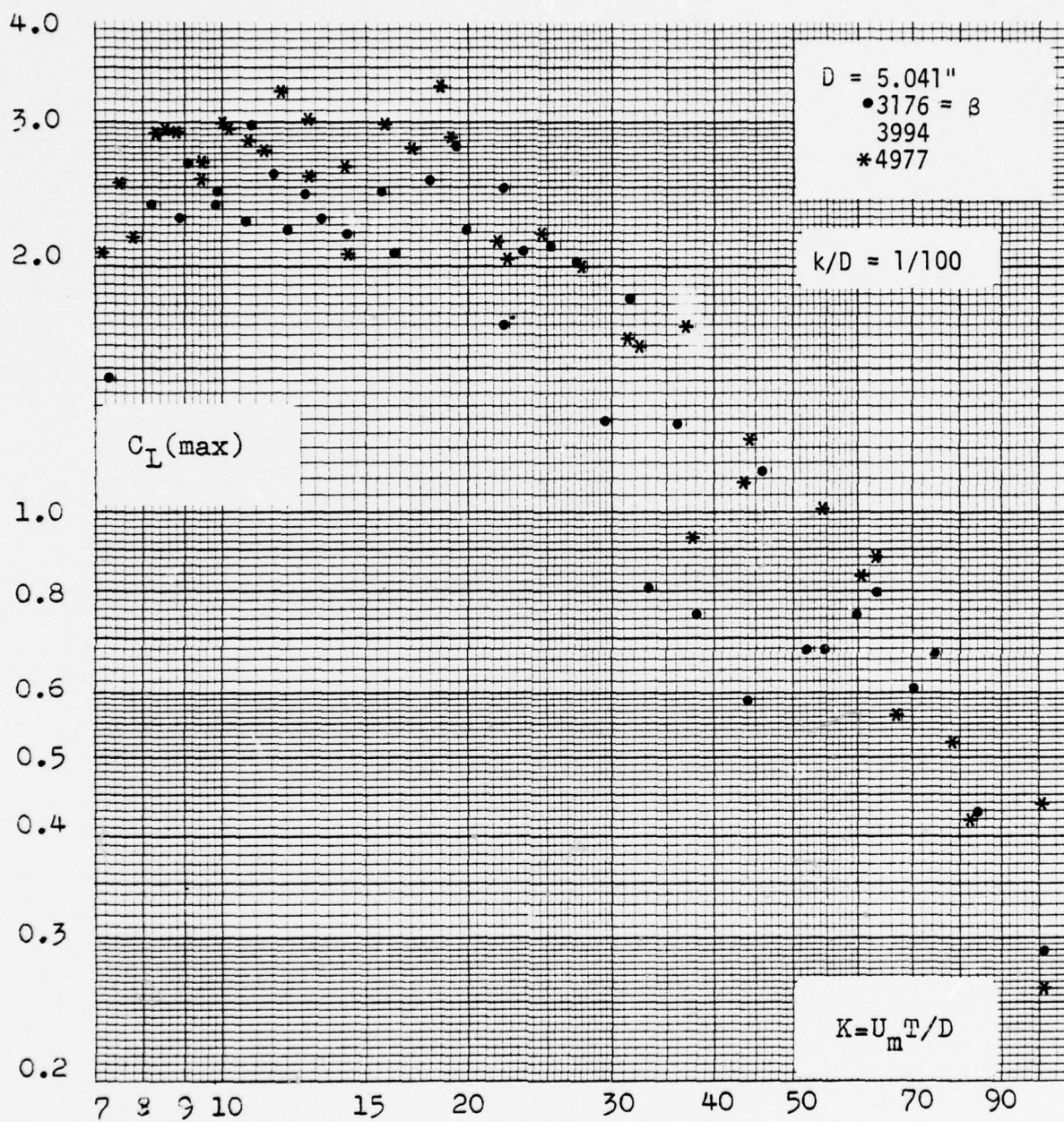


Figure 12. $C_L(\max)$ versus K for $k/D = 1/100$, 5 inch.

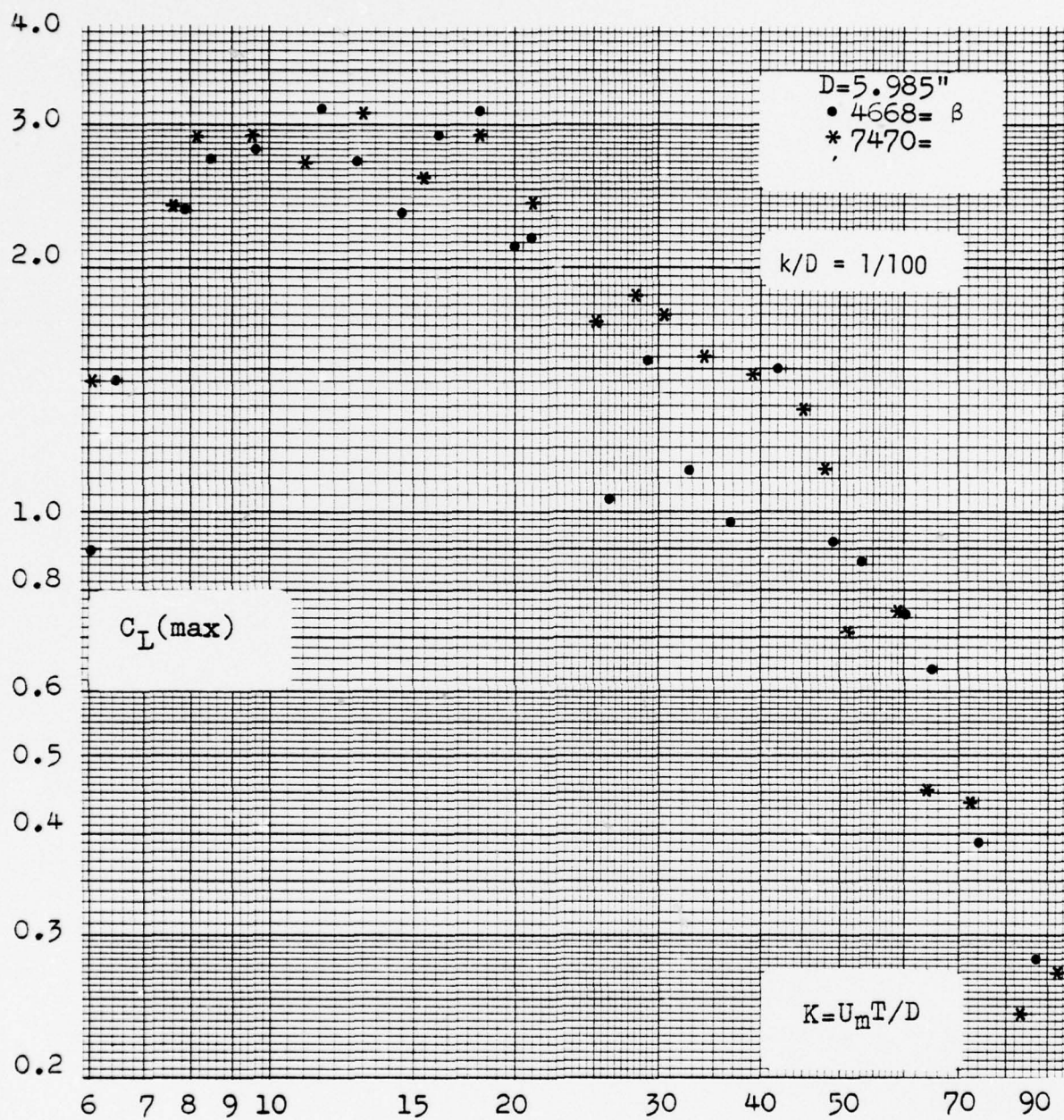


Figure 13. $C_L(\max)$ versus K for $k/D = 1/100$, 6 inch.

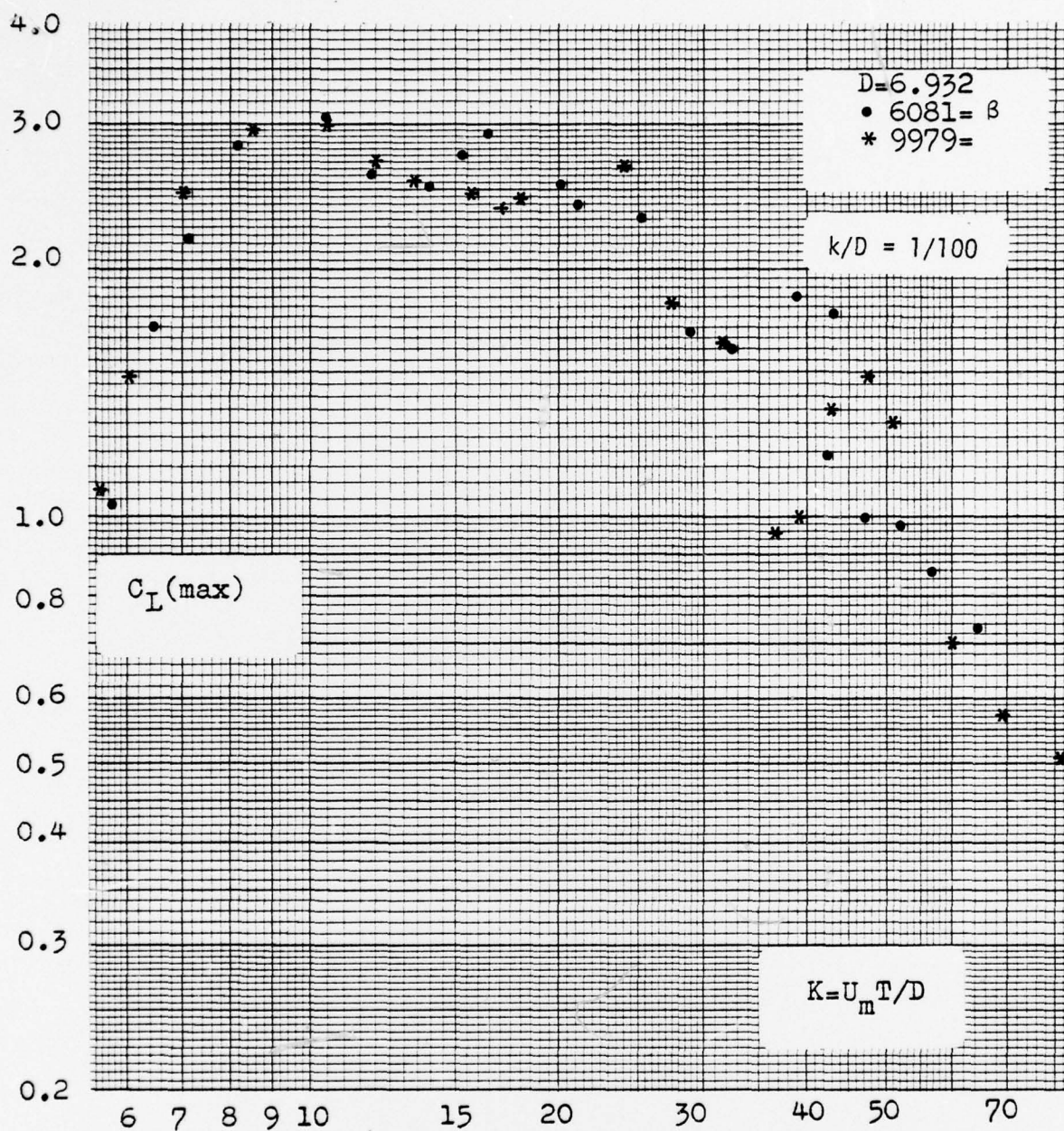


Figure 14. $C_L(\max)$ versus K for $k/D = 1/100$, 7 inch.

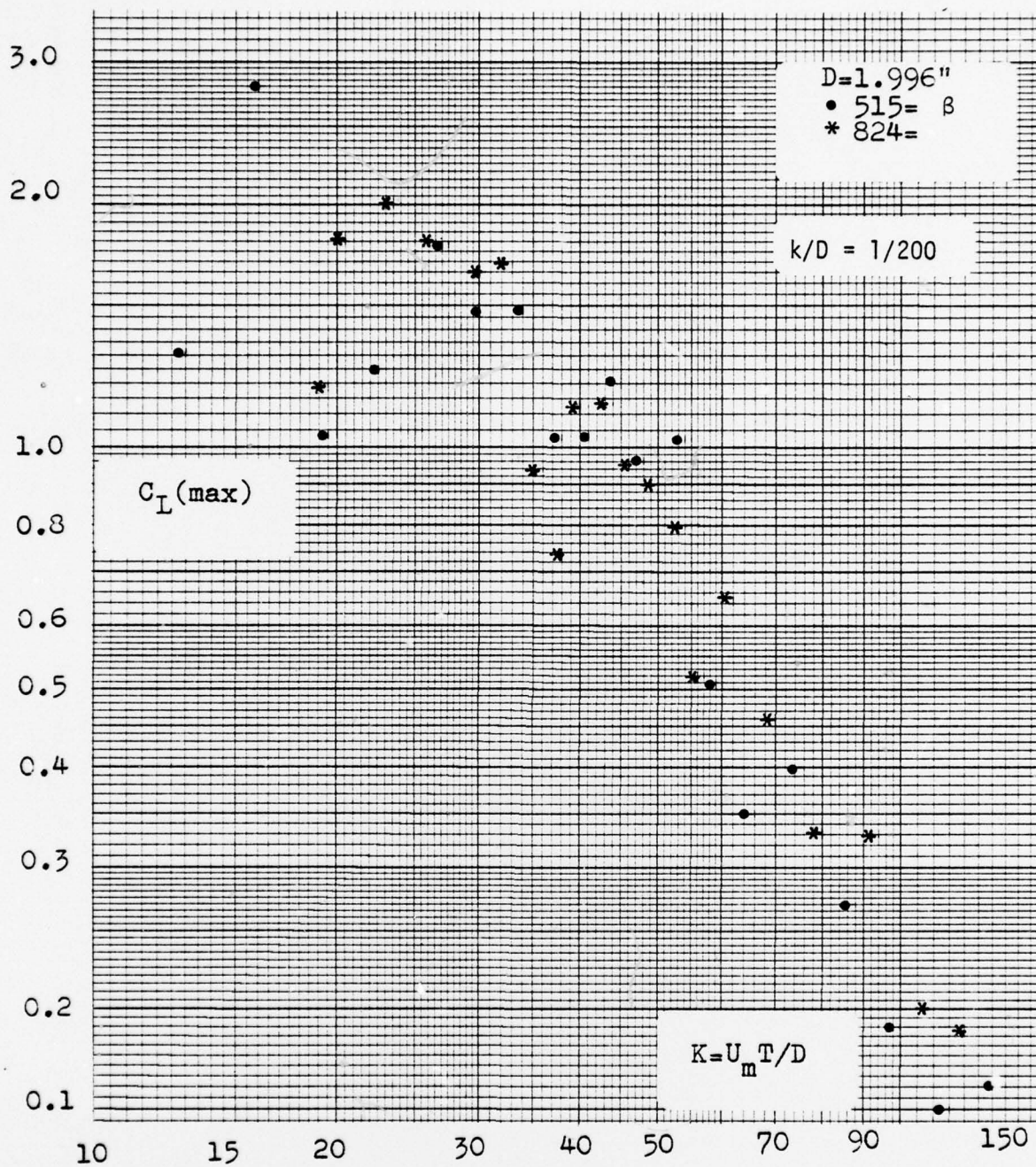


Figure 15. $C_L(\max)$ versus K for $k/D = 1/200$, 2 inch.

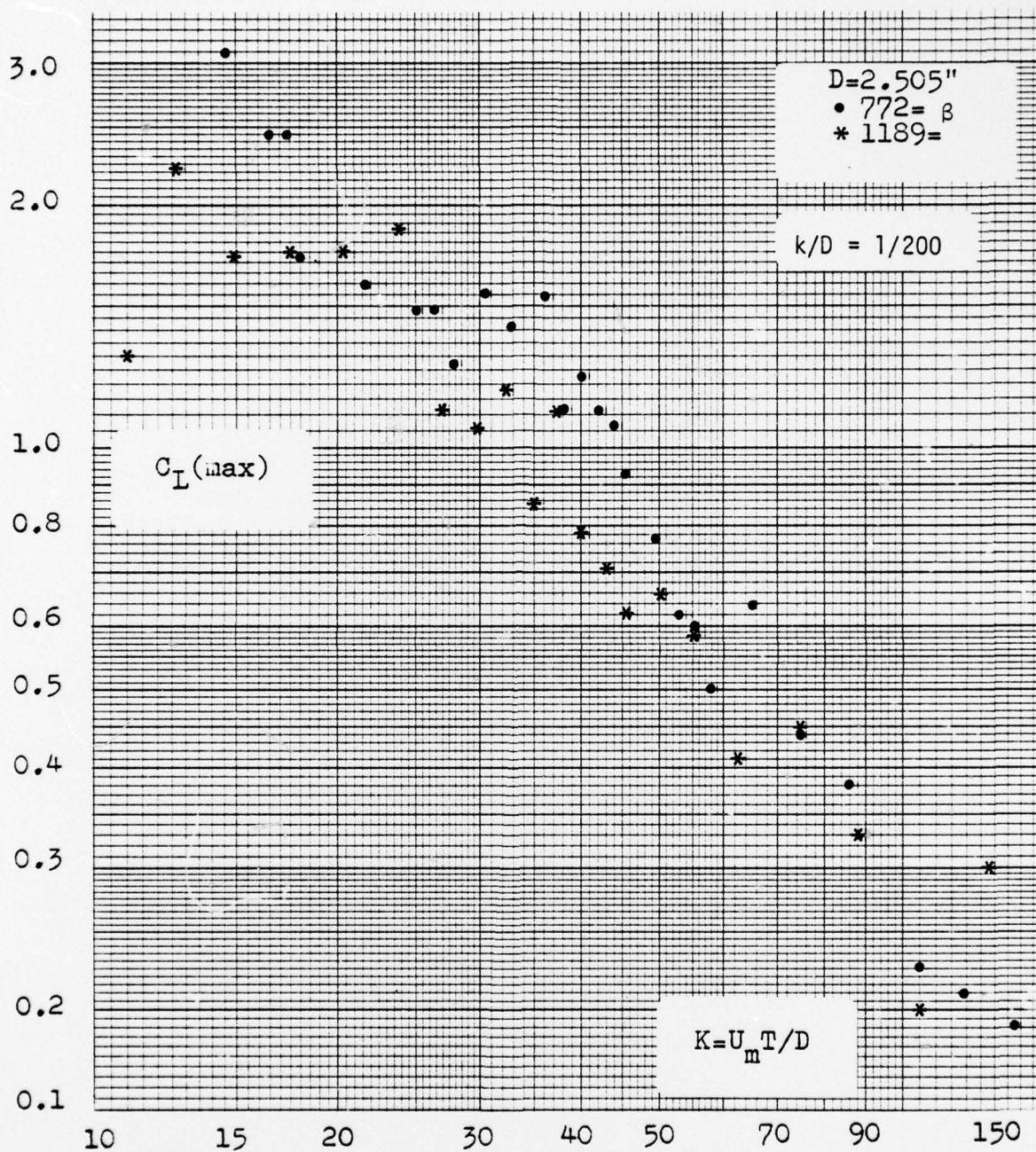


Figure 16. $C_L(\max)$ versus K for $k/D = 1/200$, 2 1/2 inch.

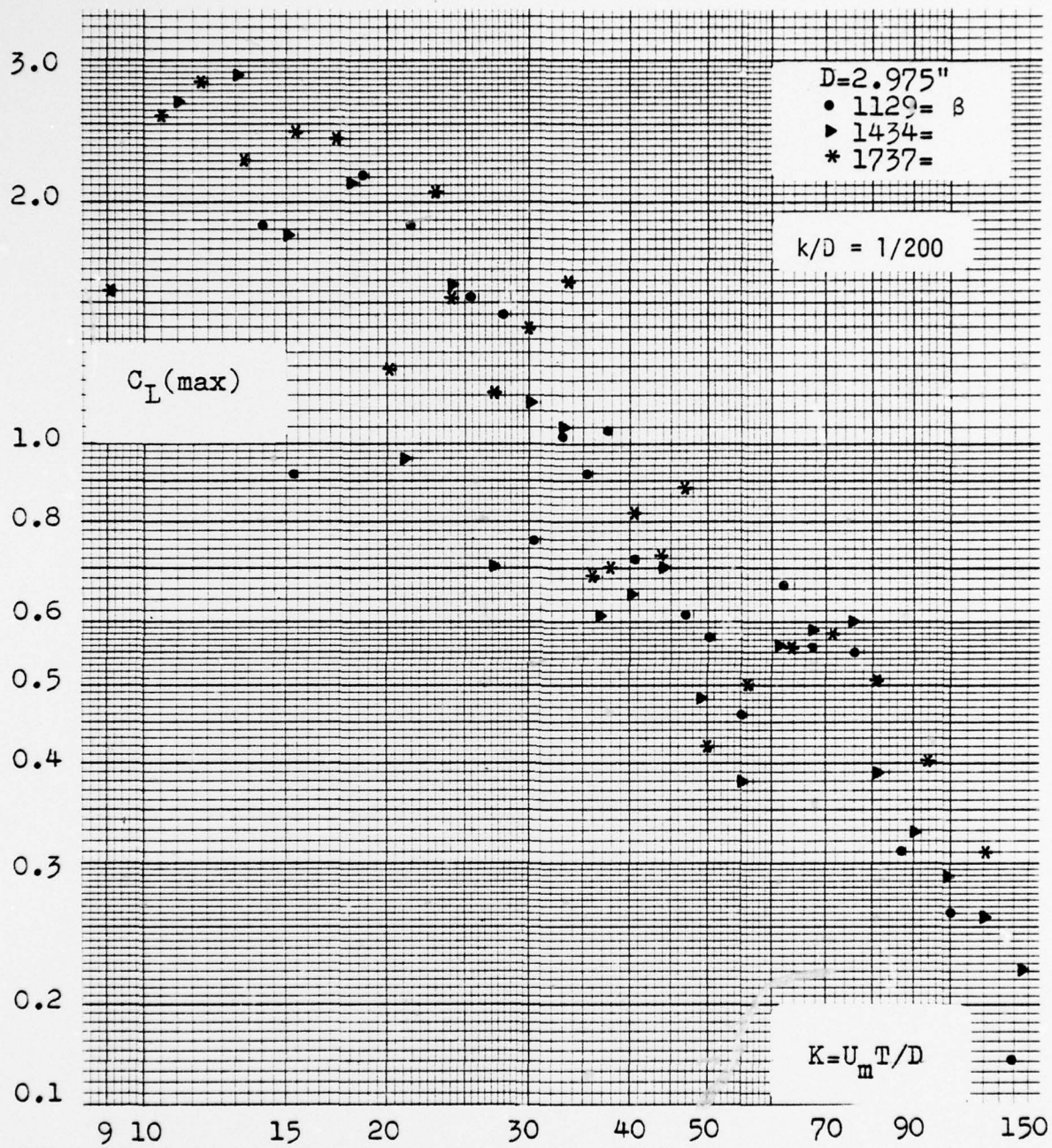


Figure 17. $C_L(\max)$ versus K for $k/D = 1/200$, 3 inch.

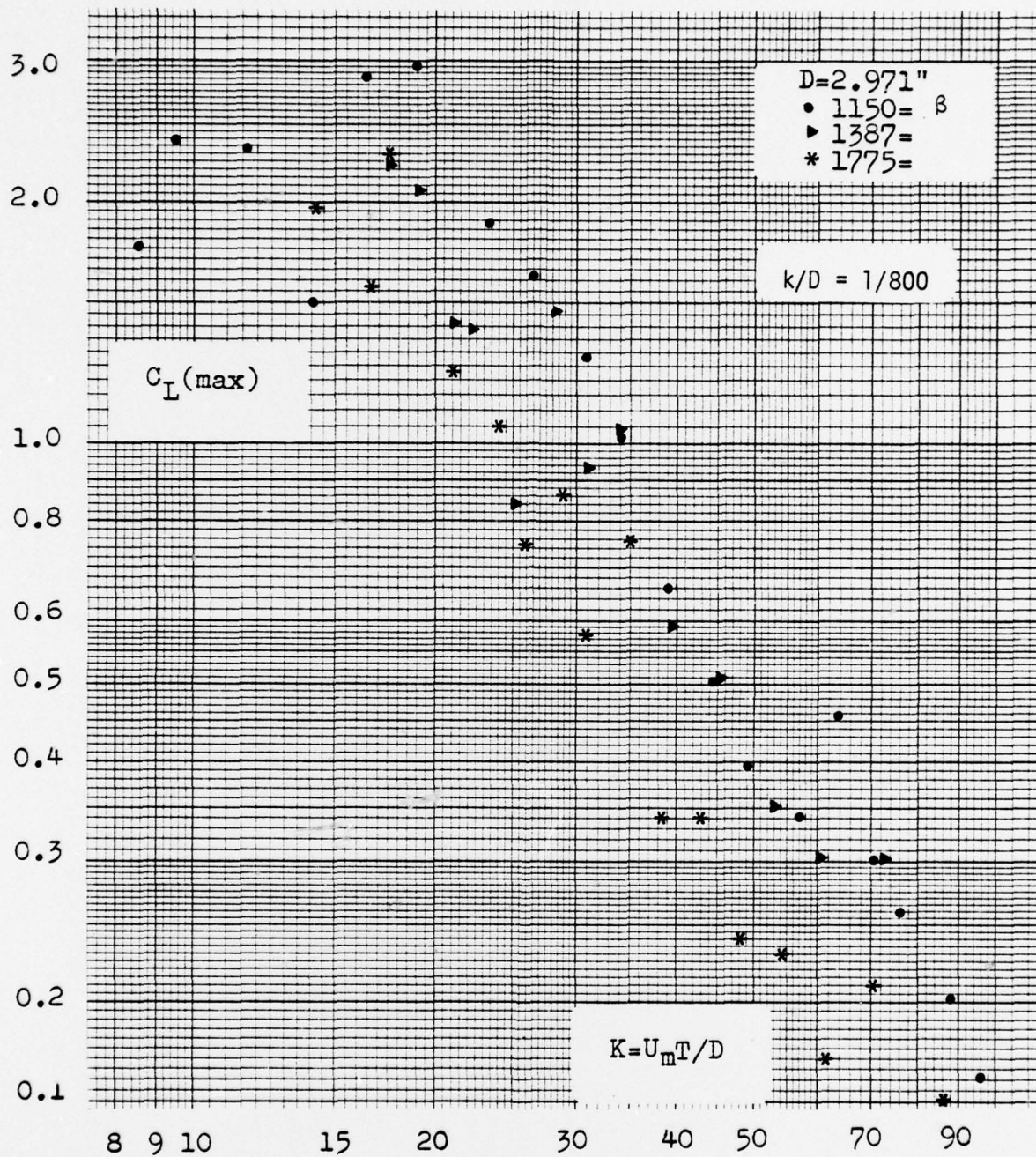


Figure 18. $C_L(\max)$ versus K for $k/D = 1/800$, 3 inch.

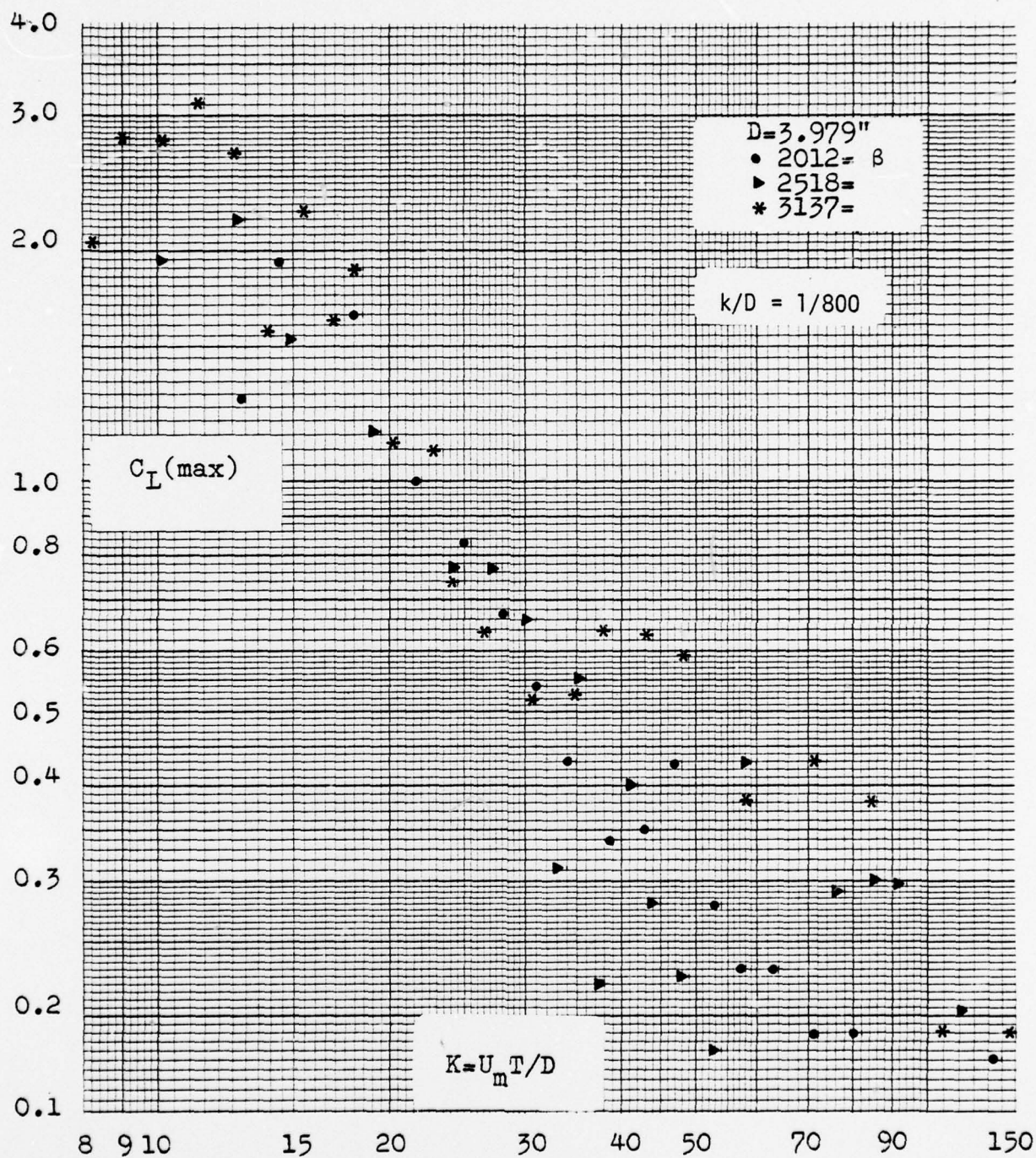


Figure 19. $C_L(\max)$ versus K for $k/D = 1/800$, 4 inch.

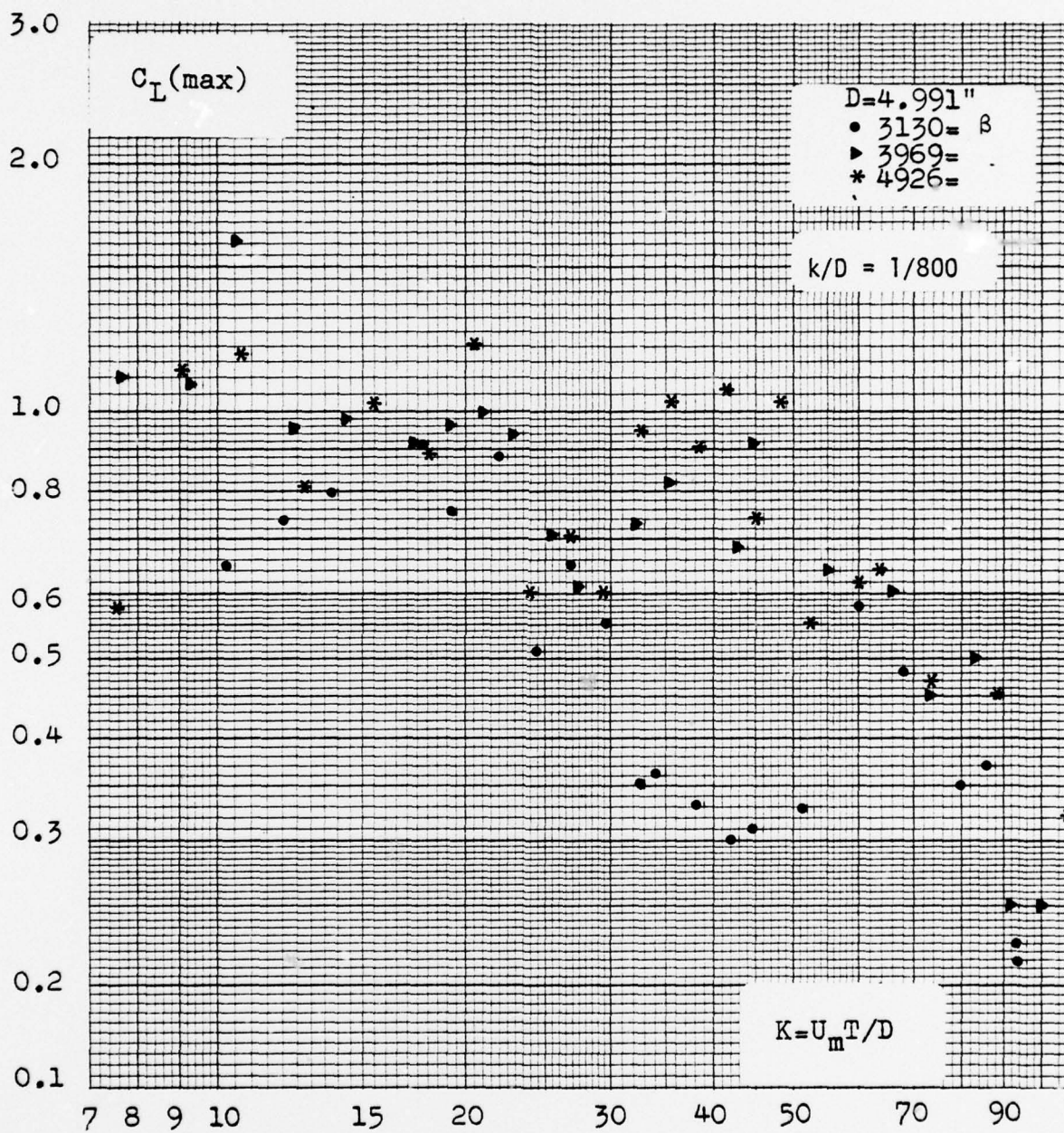


Figure 20. $C_L(\max)$ versus K for $k/D = 1/800$, 5 inch.

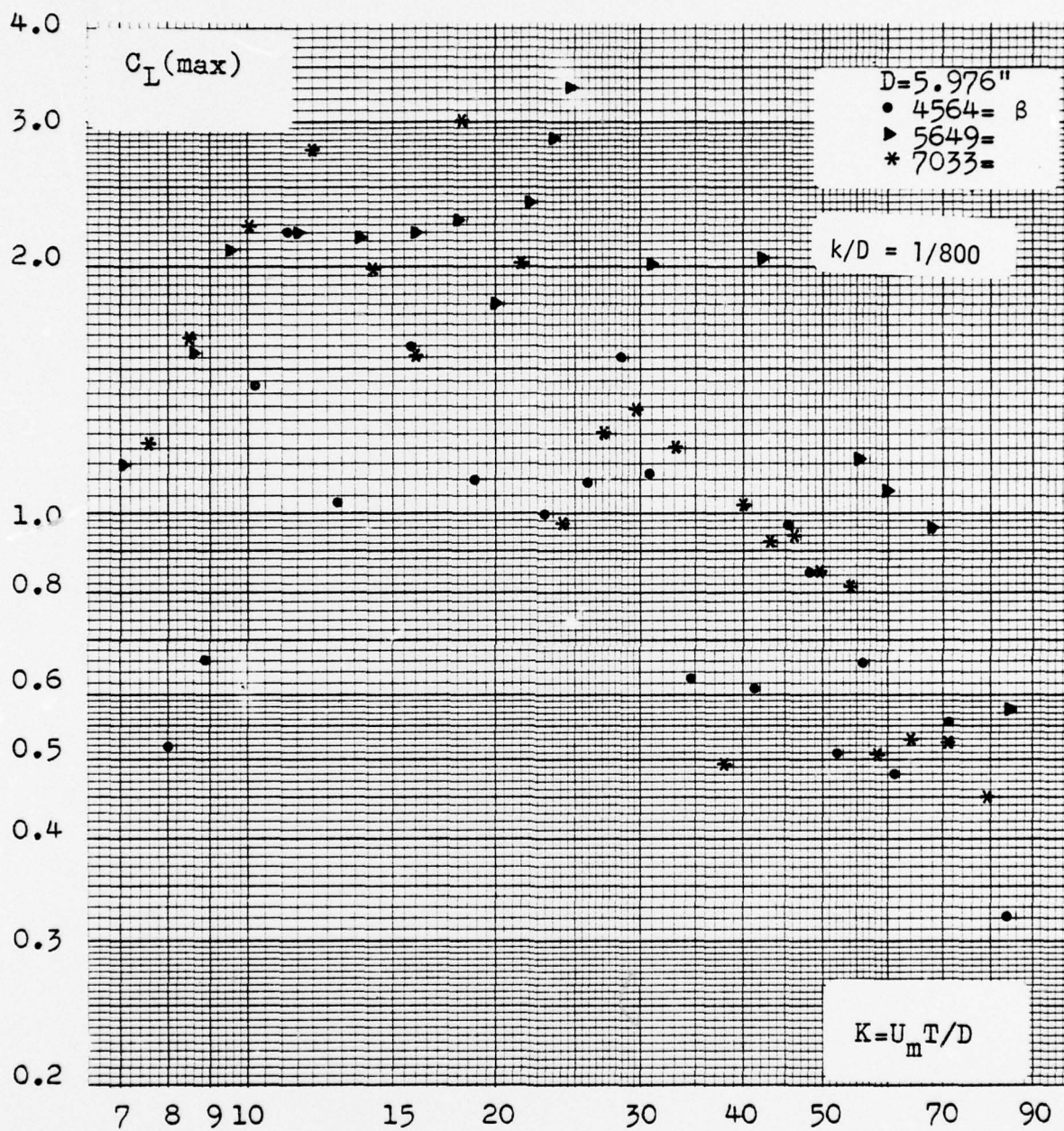


Figure 21. $C_L(\max)$ versus K for $k/D = 1/800$, 6 inch.

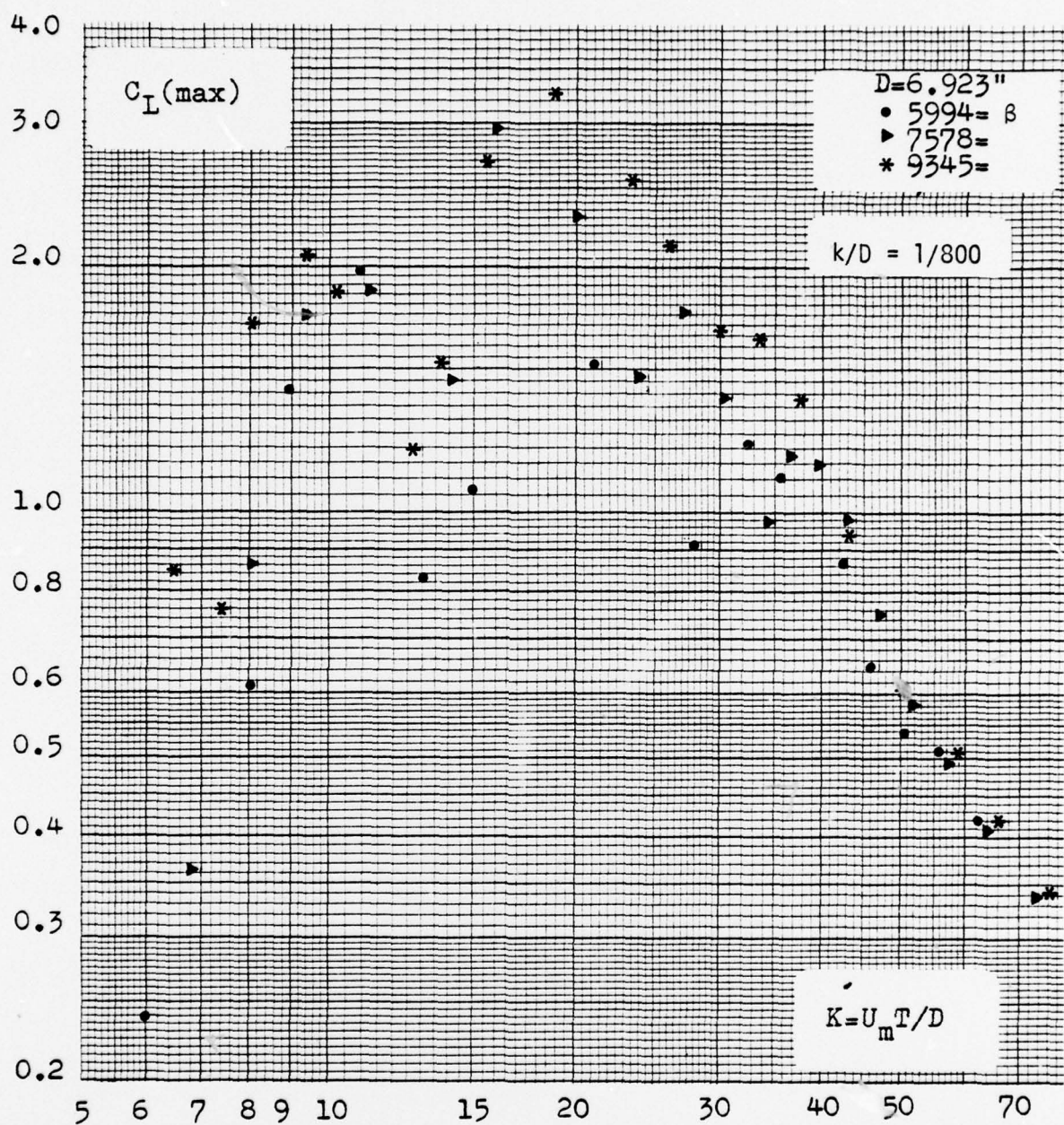


Figure 22. $C_L(\max)$ versus K for $k/D = 1/800$, 7 inch.



Figure 23. Combined plot of $C_L(\max)$ data for $k/D = 1/50$ for various values of β .

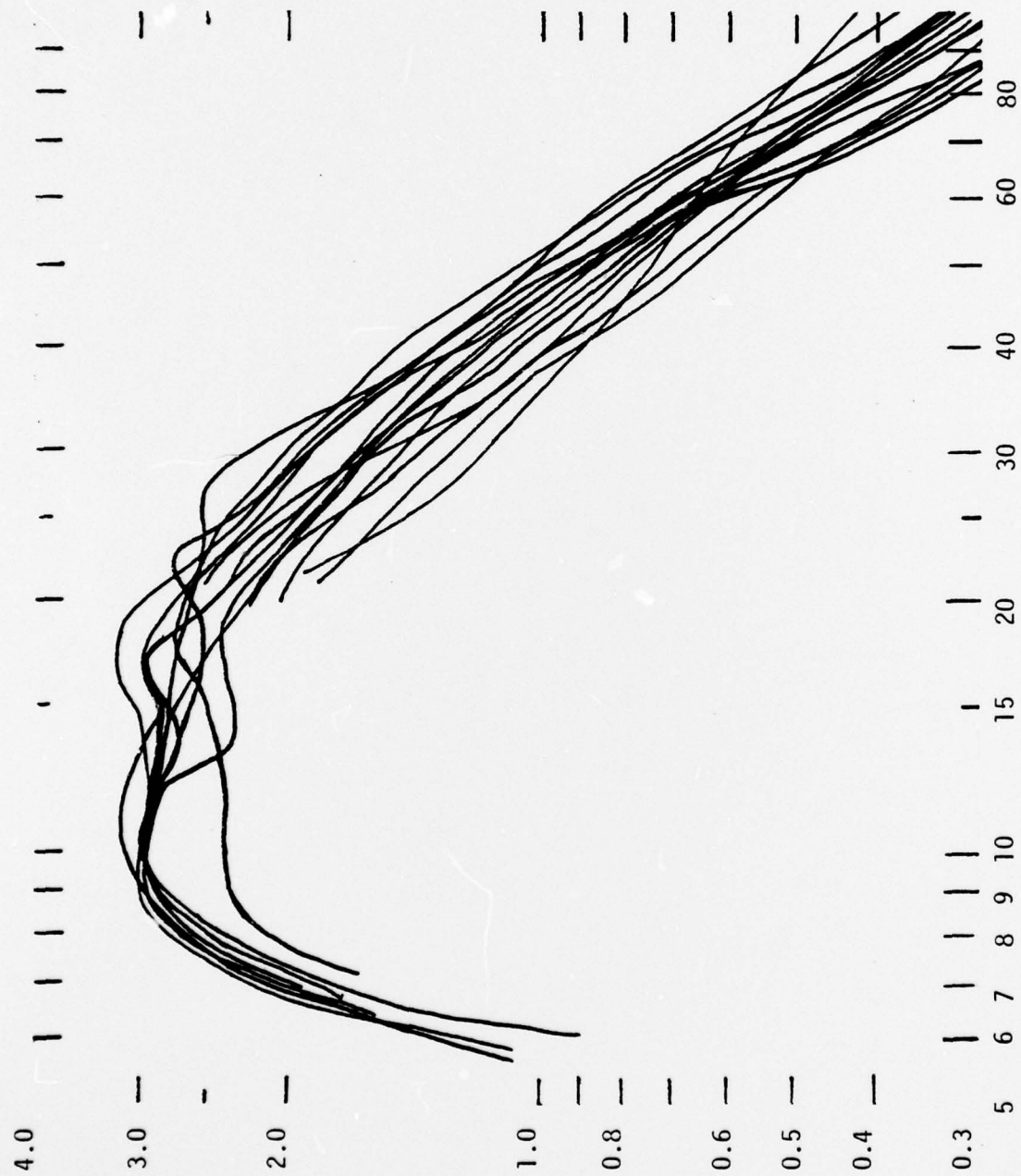


Figure 24. Combined plot of $C_L(max)$ data for $k/D = 1/100$ for various values of β .

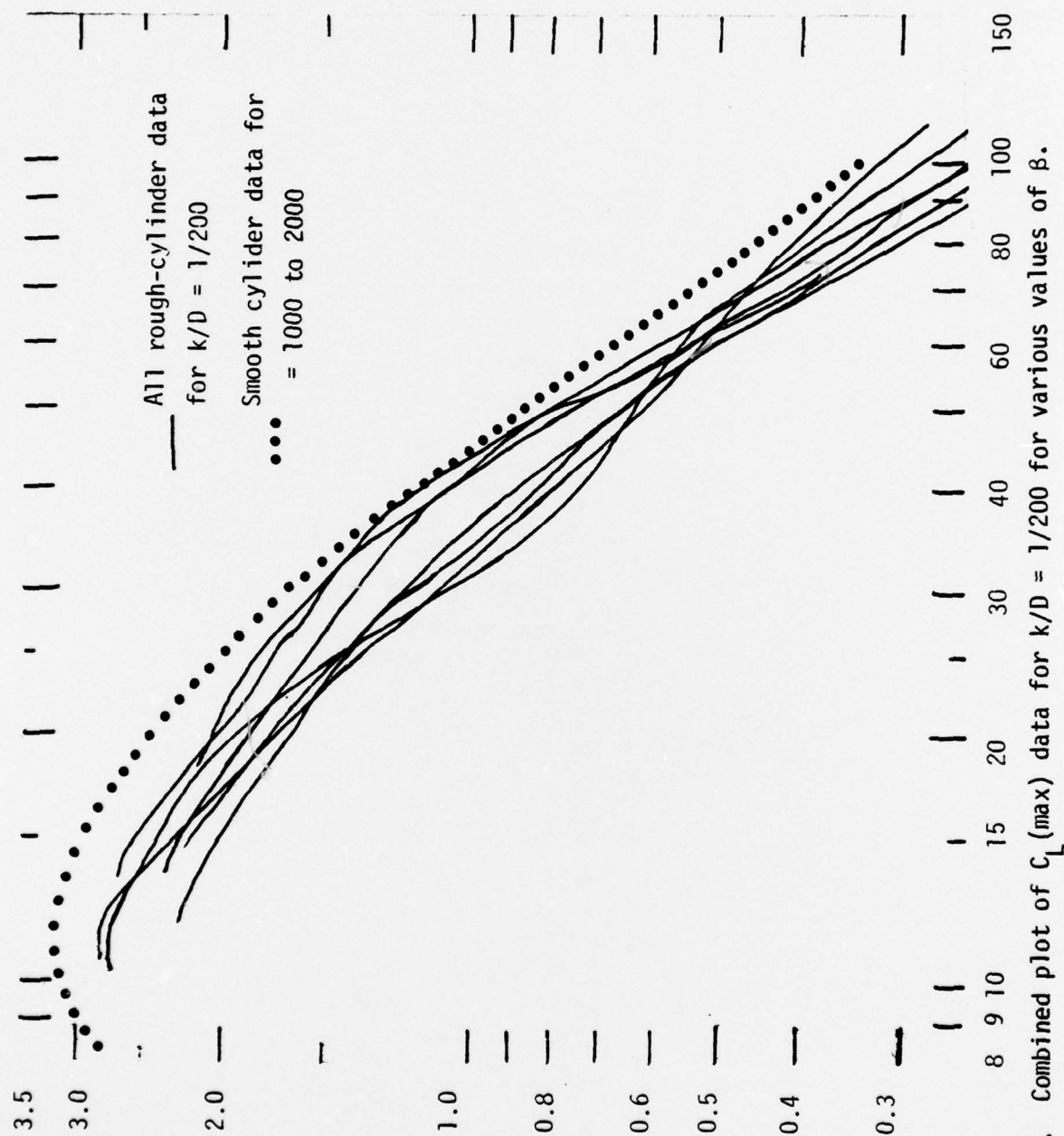


Figure 25. Combined plot of $C_{L(max)}$ data for $k/D = 1/200$ for various values of β .

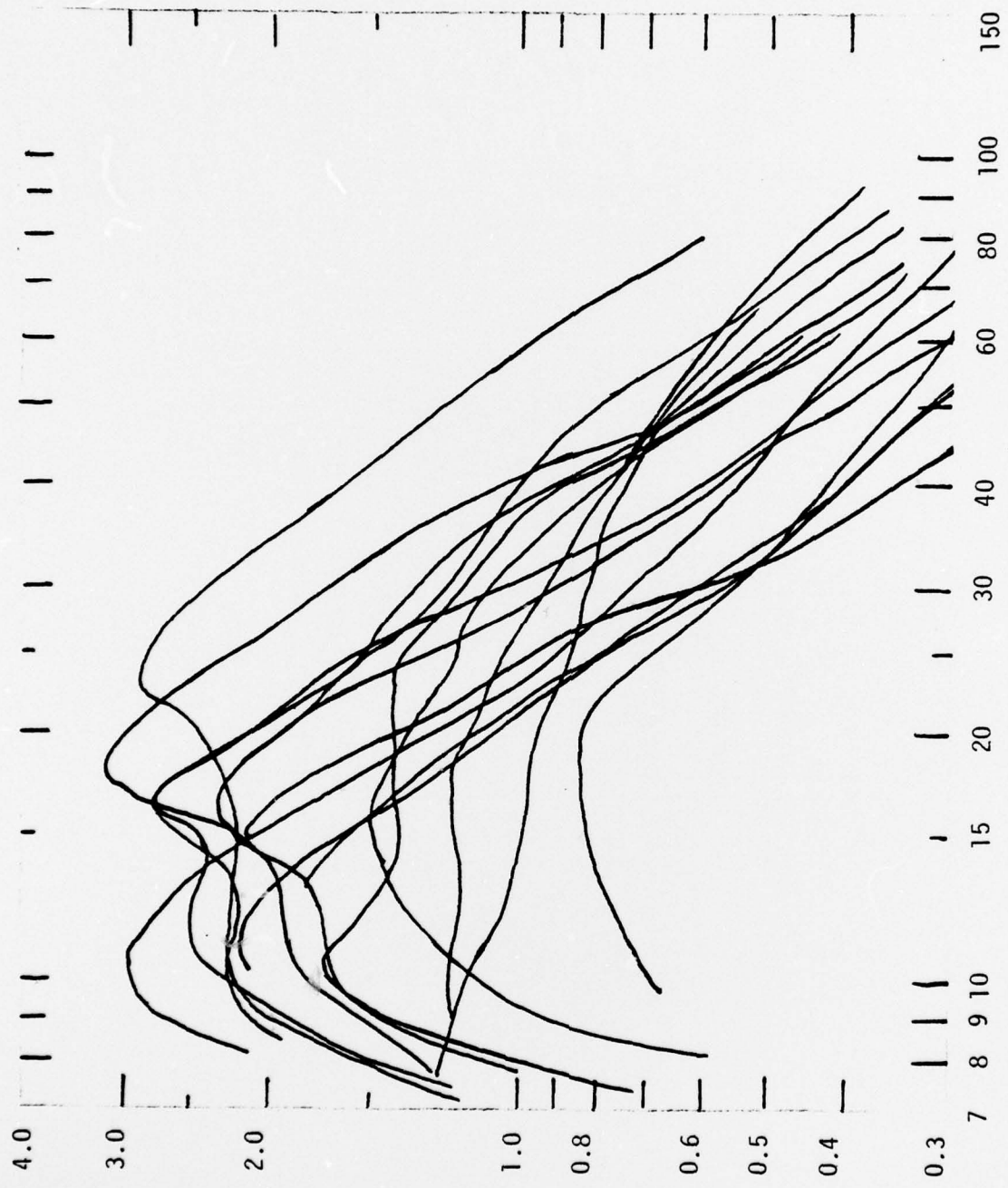


Figure 26. Combined plot of $C_L(max)$ data for $k/D = 1/800$ for various values of β .

LIST OF REFERENCES

1. Chang, K. S., "Transverse Forces on Cylinders due to Vortex Shedding in Waves," M. S. Thesis, M.I.T., 1964.
2. Bidde, D. D., "Wave Forces on a Circular Pile due to Eddy Shedding," Ph. D. Thesis, Univ. of Calif. Berkeley, Calif. Tech. Report No. HEL-9-16, 1970.
3. Wiegel, R. L. and R. C. Delmonte, "Wave-Induced Eddies and Lift Forces on Circular Cylinders," Univ. of Calif., Berkeley, Calif. Tech. Report No. HEL-9-19, 1972.
4. Mercier, J. A., "Large Amplitude Oscillations of a Circular Cylinder in a Low-Speed Stream," Ph. D. Thesis, Stevens Institute of Technology, 1973.
5. Sarpkaya, T. and O. Tuter, "Periodic Flow about Bluff Bodies, Part I: Forces on Cylinders and Spheres in a Sinusoidally Oscillating Fluid," NPS Technical Report No. NPS-59SL74091, September 1974.
6. Jones, H. K., "The Effect of a Plane Boundary on Wave-Induced Forces Acting on a Submerged Cylinder," M.S. Thesis, Naval Postgraduate School, Monterey, Calif., 1975.
7. Isaacson, M. de St. Q., "The Forces on Circular Cylinders in Waves," Ph. D. Dissertation, Univ. of Cambridge, September 1974.
8. Sarpkaya, T., "Vortex Shedding and Resistance in Harmonic Flow about Smooth and Rough Circular Cylinders at High Reynolds Numbers," Naval Postgraduate School Technical Report No. 59SL76021, Monterey, Calif. 1976.
9. Collins, N. J., "Transverse Forces on Smooth and Rough Cylinders in Harmonic Flow at High Reynolds Numbers," Mechanical Engineer Thesis, Naval Postgraduate School, Monterey, Calif., 1976.